Engrailed controls epaxial-hypaxial muscle innervation and the establishment of vertebrate three-dimensional mobility

Mohi U. Ahmed[1+], Ashish K. Maurya[2+], Louise Cheng[1,3], Erika C. Jorge[1,4], Frank R. Schubert[5], Pascal Maire[6], M. Albert Basson[1], Philip W. Ingham[2,7] and Susanne Dietrich[1,8*]

Affiliations:

[1] King's College London, Dept. of Craniofacial Development and Stem Cell Biology, Floor 27, Guy's Hospital Tower Wing, London, SE1 9RT, UK

[2]Institute of Molecular & Cell Biology, Proteos, 61 Biopolis Drive, Singapore 138673, Republic of Singapore

[3]Peter MacCallum Cancer Centre, East Melbourne, Victoria 3002, Australia

[4]Universidade Federal de Minas Gerais – Departamento de Morfologia, Av Antônio Carlos, 6627, Belo Horizonte, MG, 31270-901, Brazil

[5]Institute of Biomedical and Biomolecular Science, School of Biological Sciences, University of Portsmouth, Portsmouth PO1 2DY, UK

[6]Institut Cochin, INSERM U567, CNRS UMR 8104, Univ. Paris Descartes, Département Génétique et Développement, Equipegénétique et développement du systèmeneuromusculaire, 24 Rue du Fg St Jacques, 75014 Paris, France

[7]Dept. of Biological Sciences, National University of Singapore, 14 Science Drive 4, Singapore 117543, Republic of Singapore

[8]Institute of Biomedical and Biomolecular Science, School of Pharmacy and Biomedical Sciences, University of Portsmouth, Portsmouth PO1 2DT, UK.

[+]these authors contributed equally to the work

*Correspondence to: Susanne Dietrich, Institute of Biomedical and Biomolecular Science, School of Pharmacy and Biomedical Sciences, University of Portsmouth, Portsmouth PO1 2DT, UK; e-mail: susanne.dietrich@port.ac.uk ; phone (44) 02392 842959; fax (44) 02392 843565.

Keywords:vertebrate development and evolution, locomotion and mobility, epaxial-hypaxial muscle, muscle innervation, spinal nerves, axon guidance, dorsal ramus, ventral ramus, *Engrailed* gene, mouse, chicken, zebrafish.

Abstract

Chordates are characterised by contractile muscle on either side of the body that promotes movement by side-to-side undulation. In the lineage leading to modern jawed vertebrates (crown group gnathostomes), this system was refined: body muscle became segregated into distinct dorsal (epaxial) and ventral (hypaxial) components that are separately innervated by the medial and hypaxial motors column, respectively, via the dorsal and ventral ramus of the spinal nerves. This allows full three-dimensional mobility, which in turn was a key factor in their evolutionary success. How the new gnathostome system is established during embryogenesis and how it may have evolved in the ancestors of modern vertebrates is not known.

Vertebrate *Engrailed* genes have a peculiar expression pattern as they temporarily demarcate a central domain of the developing musculature at the epaxial-hypaxial boundary. Moreover, they are the only genes known with this particular expression pattern. The aim of this study was to investigate whether *Engrailed* genes control epaxial-hypaxial muscle development and innervation.

Investigating chick, mouse and zebrafish as major gnathostome model organisms, we found that the *Engrailed* expression domain was associated with the establishment of the epaxial-hypaxial boundary of muscle in all three species. Moreover, the outgrowing epaxial and hypaxial nerves orientated themselves with respect to this *Engrailed* domain. In the chicken, loss and gain of *Engrailed* function changed epaxial-hypaxial somite patterning. Importantly, in all animals studied, loss and gain of *Engrailed* function severely disrupted the pathfinding of the spinal motor axons, suggesting that *Engrailed* plays an evolutionarily conserved role in the separate innervation of vertebrate epaxial-hypaxial muscle.

Introduction

Mobility is a key feature of animals and is fundamental to their evolutionary success. In vertebrates, mobility relies on the action of skeletal muscles and their innervating nerves, and it underlies the ability to breathe, eat, explore the environment, even to control the sense organs. Terrestrial vertebrates use their limb musculature and cognate nerves to move about. Before conquering land 360 million years ago, however, vertebrates spent some 200 million years in the water, employing swimming as their primitive form of locomotion, powered by the undulation of the body and tail. Such movement is accomplished by the alternating contraction of muscle blocks, or myotomes, that act as antagonists on either side of the animal. Derivatives of these muscles are still present in terrestrial vertebrates to date, supporting the action of the limbs, lifting the body of the ground and in humans, allowing upright stance (reviewed by Clack, 2002).

Bilateral series of muscle blocks on either side of the axial midline are not a feature of vertebrates alone. They are also found in tunicate larvae (urochordates) albeit in a secondarily reduced form, and in amphioxus (cephalochordates), and hence are typical for chordates. Importantly, in invertebrate chordates as well as jaw-less agnathan/cyclostome vertebrates such as the lamprey, the muscle segments are dorsoventrally continuous, with muscle fibres running parallel to the main body axis. This arrangement facilitates side-to-side movement of the body and tail in a horizontal plane, but restricts movement in the vertical plane. By contrast, modern jawed vertebrates (crown group gnathostomes encompassing all living gnathostomes and their closely related extinct relatives) are well capable of side-to-side as well as upwards-downwards movements, as best displayed by eels and by all land-living tetrapods. The anatomical basis of this superior mobility is a subdivision of body muscles into distinct dorsal (epaxial) and ventral (hypaxial) elements, separated by a connective tissue sheet called horizontal myoseptum (non-tetrapods) or thoracolumbar fascia (tetrapods). Epaxial and hypaxial muscle contraction is controlled separately by distinct populations of motor neurons, which target the muscles via the dorsal and ventral ramus of the spinal nerves. This arrangement allows the epaxial and hypaxial muscles to contract independently. Consequently, not only muscles on the left and right side of the body axis but also the dorsal and ventral muscles can act as antagonists, thus providing full three-dimensional mobility (reviewed by Fetcho, 1987).

As the epaxial-hypaxial subdivision and innervation of muscle is a synapomorphy (shared derived character) of extant jawed vertebrates, the ancestor of today's gnathostomes must at some point have evolved a distinct developmental mechanism that facilitated the establishment of the new trait. However, what this mechanism was, and whether it is still traceable to date, is not known. Genetic and transplantation experiments have established that signals from the paraxial mesoderm influence the position-dependent specification of motor neuron subtypes both in amniotes and anamniotes (Appel et al., 1995; Ensini et al., 1998). Thereafter, motor neurons are cell-autonomously set up to recognise their specific epaxial-hypaxial (in fish also central) targets (reviewed by Lewis and Eisen, 2003; Shirasaki and Pfaff, 2002). Yet microsurgical ablation experiments in chicken (Tosney, 1987), genetic ablation experiments in the mouse (Kablar and Rudnicki, 1999) and a host of studies on paraxial mesoderm mutants in the zebrafish (reviewed by Lewis and Eisen, 2003) showed that the developing musculature is crucial for spinal nerve outgrowth, ramus formation and motor neuron survival. This suggests that regulatory molecules reside within the muscle and are offered to the outgrowing nerves.

A number of axon guidance molecules have been identified that are present when segmental muscle blocks develop. In amniotes, specifically Semaphorin3A, Ephrins and chondroitin sulphate

proteoglycans have been identified as chemorepulsive molecules, but these affect both the dorsal and the ventral ramus and are mainly involved in defining the rostro-caudal position of the spinal nerves within a segment (reviewed by Bonanomi and Pfaff, 2010). Fibroblast growth factors (FGFs) have been identified as attractants for the axons of the neurons that contribute to the dorsal ramus. However, FGFs are expressed in a dorsoventrally continuous stripe throughout the middle of the myotome (Shirasaki et al., 2006) encompassing both the epaxial as well as the hypaxial domains. In the zebrafish, sema3aa, sema3ab, robo3 and a number of extracellular matrix molecules have been implicated in axonal repulsion, yet attraction to intermediate (choice points) and ultimate motor neurons targets is even more unclear than in amniotes (Halloran et al., 2000; Hilario et al., 2010; Sato-Maeda et al., 2006; Schneider and Granato, 2006); (reviewed by Lewis and Eisen, 2003). It has been proposed that differential responses of epaxial-hypaxial neurons to the same axon guidance molecule may be regulated intrinsically, elicited by the differential expression of receptors (Sato-Maeda et al., 2006; Shirasaki et al., 2006). Yet an evolutionarily conserved, basic mechanism that allows epaxial-hypaxial muscle to attract its cognate innervation remains to be discovered.

In all jawed vertebrates analysed so far, including amniotes (mouse, chicken; Cheng et al., 2004; Spörle, 2001) and anamniote tetrapods (Xenopus; Grimaldi et al., 2004) that represent the sarcopterygian lineage, teleost fish that represent the actinopterygian lineage (zebrafish; Devoto et al., 1996; Ekker et al., 1992; Hatta et al., 1991) and the spotted dogfish that represents chondrichthyans (Tanaka et al., 2002), the homeodomain transcription factor and short-range signalling molecule Engrailed is expressed in the centre of the developing muscle blocks and demarcates the site of the future epaxial-hypaxial divide. In the zebrafish, the *Engrailed* expressing cells are morphologically distinct, organise the formation of the horizontal myoseptum and serve as intermediate targets for the pioneer motor axons which define the axonal path for the secondary motorneurons that, in turn, innervate the muscles of both the larvae and adults (Beattie and Eisen, 1997), reviewed by (Lewis and Eisen, 2003). In amniotes, *Engrailed* expressing cells are morphologically inconspicuous. Yet they demarcate the epaxial side of the epaxial-hypaxial interface and sort from the hypaxially located *Engrailed*-negative cells, thereby forming a compartment boundary (Cheng et al., 2004). Notably, somitic *En1/eng* expression is controlled by similar signals both in zebrafish and amniotes (Cheng et al., 2004; Currie and Ingham, 1996; Dolez et al., 2011; Maurya et al., 2011). We therefore hypothesised that *Engrailed* may have a conserved function for epaxial-hypaxial muscle development and innervation and may have facilitated the evolution of vertebrate 3D-mobility.

In this study, we investigated the relationship of epaxial-hypaxial muscle innervation and *Engrailed* expression in the mouse, the chicken and the zebrafish, representing both the sarcopterygian and antinopterygian lineages of jawed vertebrates. We show that in all animals, spinal motor axons show stereotypical projection patterns towards or away from the *Engrailed* expression domain before muscle becomes morphologically segregated into epaxial-hypaxial domains. Gain- and loss-of-function experiments revealed that *Engrailed* function controls muscle patterning and, importantly, is required for the correct innervation of dorsal and ventral body muscle.

Materials and Methods

Mouse husbandry and mouse embryos

All mice were maintained and bred according to UK Home Office license regulations. Noon of the day a vaginal plug was detected was considered E0.5. The *En1*$^{cre/+}$ (Kimmel et al., 2000) mouse line was kindly provided by Gail Martin (University of California, San Francisco). The mice were crossed with Rosa26-lacZ mice (Soriano, 1999) to lineage-trace *En1* expressing cells and intercrossed to produce homozygous *En1*$^{cre/cre}$ (*En1*$^{-/-}$) embryos. Embryos were dissected in PBS and fixed in 4% PFA/PBS overnight at 4°C. Embryonic yolk sac DNA was used to genotype *En1* mutant mice by PCR using the following primers: *En1* wildtype allele, 5'-CACCGCACCACCACCTTTTTC-3' and 5'-TCGCATCTGGAGCACACAAGAG-3'; *En1* mutant allele, 5'-TAAAGATATCTCACGTACTGACGGTG-3' and 5'-TCTCTGACCAGAGTCATCCTTAGC-3'. The wildtype and mutant band sizes were 238bp and 300bp, respectively.

Chicken embryos

Fertilised hen's eggs were purchased from Henry Steward Ltd, Royston, following (Ahmed et al., 2006; Alvares et al., 2003; Cheng et al., 2004; Mootoosamy and Dietrich, 2002) for incubation and embryo preparation. Embryos were staged according to (Hamburger and Hamilton, 1951).

Zebrafish lines, husbandry and embryos

Adult fish were maintained on a 14 hour light/10 hour dark cycle at 28°C in the AVA (Singapore) certificated IMCB Zebrafish Facility. Wildtype zebrafish strains in this study were AB and TL; transgenic strains were *Tg*(*eng2a:eGFP*)^{i233},*Tg*(*actc1b:GAL4*)^{i269} (Maurya et al., 2011). Embryos were injected at 1-2 cell stage and fixed at 36 hpf with 4%PFA for 2 hours at room temperature or overnight at 4 °C, washed in PBS and stored in methanol at -20 until further use.

Molecular constructs and morpholinos

The avian *En1* expression construct was made by cloning the open reading frame (orf) of mouse *En1* into the ClaI site of the bi-cistronic pCaβ vector (Alvares et al., 2003) which contains an internal ribosomal entry site (IRES) followed by the open reading frame for *GFP*. For the dominant negative construct, the portion of the mouse *En1* orf located 5' of the EH1 domain was amplified using adaptors with ClaI and MfeI sites, respectively. The VP16 fragment was amplified using adaptors with MfeI and NheI sites. The mouse *En1* orf 3' of the EH1 domain was amplified using Nhe and EcoRI containing adapters. All fragments were cloned into the Cla-EcoRI sites of pCaβ. For the zebrafish expression constructs, the zebrafish *eng2a* orf was amplified using EcoRI containing adaptors and cloned into the EcoRI site of the bicistronic UAS-UAS-tRFP-Tol2 vector (Maurya et al., 2011). The mouse *En1* orf was excised from the pCaβ vector using XbaI-AflIII, blunt-ended with T4 DNA polymerase, and cloned into the blunt-ended EcoRI sites of this vector. All constructs were confirmed by sequencing.

Morpholinos were as follows

Eng1a-ATG	TGACCCCGCCGCTGATCCTCCATAA;
Eng1a-I1-E2-Splice	GCCTTGTGTGGAGACAACAATGAAA;
Eng1b-ATG	TTTTGATCCTTTTGCTCGTCCATGA;
Eng1b-E1-I1-Splice	TTAAGAAACTAGCGCCTTACCAGAT;
Eng2a-ATG	TTGCGCTCTGCTCATTCTCATCCAT;
Eng2a-E1-I1-Splice	AAATAGAGGTAAGCGTACCTGACGA;

Control Morpholinos:

Sfrp2-ATG	CGTGGGTTACTGAATTGTTCACTGT;
Sfrp2-E1-I1	TGACTTGAAACTTTTCGTACCTTCC.

The injection of morpholinos and expression constricts into fish embryos was performed as described in (Maurya et al., 2011).

In vivo somite electroporation

The somitocoels of 2-4 flank somites at E2.5/ stage HH15-16 were injected with 2-4μg/μl DNA, 0.1% Fast Green (Sigma) in PBS as detailed in (Alvares et al., 2003) and each somite was exposed to 1-2 20ms rectangular pulses of 18V generated by a Intracept TSS10 electroporator (Intracel). For hypaxial electroporations, a 0.5 mm platinum wire (positive electrode) was placed lateral to the somites, a 0.1mm flame-sharpened tungsten wire (negative electrode) was placed into the neural

tube; the epaxial-central domain was targeted by placing the tungsten wire below and the platinum wire above the somite. Embryos were collected 24 or 48 hours post-electroporation and fixed in 4% PFA/PBS at 4°C overnight. Embryos displaying GFP-dependent fluorescence were processed for further analyses. For co-electroporation experiments, simultaneous uptake of constructs was tested, electroporating an equimolar mix of the RFP and the standard GFP expressing pCaβ vectors and analysing for red and green fluorescence in the same cell. Specificity and efficacy of the siRNA mediated knock down was tested by co-electroporating pCaβ/GFP and a siRNA construct expressing RFP targeted against GFP and assaying for the presence of red and the absence of green fluorescence, respectively (Supplementary material 1).

In situ hybridisation, immunohistochemistry and sectioning

The protocols for the *in situ* hybridisation, immunohistochemistry and vibratome sectioning of chicken and mouse embryos are described in (Ahmed et al., 2006; Cheng et al., 2004; Mootoosamy and Dietrich, 2002). The protocols for immunohistochemistry and sectioning of zebrafish embryos are described in (Elworthy et al., 2008). Details of antisense probes: mouse *En1*, *Myf7*, *Pax7* (Dietrich, 1999; Logan et al., 1992); chicken *Alx4*, *En1*, *EphA4*, *Follistatin*, *Lbx1*, *Myf5*, *MyoD*, *MyoR (Msc)*, *Pax3*, *Pax7*, *R-Cadherin (Cdh4)*, *Sim1*, *Six1* (Ahmed et al., 2006; Berti et al., 2015; Cheng et al., 2004; Dietrich et al., 1998; Mootoosamy and Dietrich, 2002); the chicken *En1* 3' UTR probe was obtained by linearising the template described by (Logan et al., 1992) with ClaI and transcription with T3 RNA polymerase. Antibodies: monoclonal mouse anti-neurofilament antibody RMO-270 (Zymed Laboratories; 1:3000), monoclonal mouse anti-β3 tubulin antibody Tuj1 (Abcam; 1:1000), znp1 antibody detecting synaptotagmin 2 (DHSB; 1:2000), rabbit polyclonal ant-GFP antibody (Life technology; 1;1000), rabbit polyclonal anti-tRFP (Evrogen; 1:750), peroxidase-conjugated goat anti-mouse antibody (Dako; 1:200), AlexaFluor488-labelled anti-mouse IgG and AlexaFluor568-labelled anti-rabbit IgG antibodies (Invitrogen, 1:200).

Photomicroscopy

Images of chicken and mouse specimens were captured by a Zeiss AxioCam digital camera (Imaging Associates) using a Zeiss Axioskop 2 microscope with Nomarski optics or fluorescence, except images in Fig.3C-F that were captured using a Zeiss StereoLumar V12 microscope. Images of zebrafish specimen were captured using a 60× oil immersion objective on an Olympus Fluoview 1000 confocal microscope using Olympus FV10-ASW software; fluorescent axon stainings in the mouse were captured on a Zeiss LSM710 confocal microscope, using ZEN software. Images were analysed using ImageJ software (http://rsbweb.nih.gov/ij/). For 3D rotations, the z-stacks of confocal images were

loaded into the Volocity software. Panels of images were assembled and edited using Adobe Photoshop 9 CS.

Results

1. Relationship of amniote *En1* expression and the epaxial-hypaxial innervation of muscle

Skeletal muscle develops from undifferentiated blocks of paraxial mesoderm, known as somites (reviewed by Bryson-Richardson and Currie, 2008; Buckingham, 2006). In amniotes, the somites differentiate into the ventrally located, vertebral column-building sclerotome and the dorsally located dermomyotome which delivers both the body musculature and the dorsal dermis. Muscle formation begins when the dermomyotome releases post-mitotic, differentiating cells first from its dorsomedial and ventrolateral lips, then from its rostrocaudal lips. The cells settle beneath the dermomyotome and form the early myotome. Later, in the chicken embryo at day 3.5-4 of its 21 days of development, the dermomyotome disperses, with mitotically active embryonic muscle stem cells populating the myotome to deliver the bulk of the fetal and adult musculature as well as adult muscle stem cells, and with dermal cells settling underneath the epidermis to contribute to the developing skin (reviewed by Bryson-Richardson and Currie, 2008; Buckingham, 2006). We previously established the *Engrailed1* (*En1*) gene as a marker for the chicken epaxial somitic dermomyotome where *En1*-expressing cells form a compartment boundary with the neighbouring hypaxial cells expressing *Sim1* (Cheng et al., 2004). Moreover, we showed that the developing muscle stem cells continue to express *En1* when they populate the myotome, thereby establishing the molecular epaxial-hypaxial subdivision in the myotome (Ahmed et al., 2006). The process of somite innervation commences when the ventrally exiting motor axons and the sensory axons derived from the dorsal root ganglion project into a joined spinal nerve (reviewed in Bonanomi and Pfaff, 2010; Fetcho, 1987). However, whether somite innervation relates to the expression domain of *En1* was not known. To set the stage, we investigated the time and pattern by which the chicken dorsal and ventral ramus target the flank myotomes (Fig.1). To explore the relationship of epaxial-hypaxial muscle innervation with the molecular and physical subdivision of the myotome, we performed double-staining experiments at the time when both the dorsal and ventral rami of the spinal nerves make contact with the myotome, detecting the expression of *En1*, the hypaxial marker *Sim1*, the myotomal marker *Myf5* and the dermomyotomal and muscle stem cell marker *Pax7* (Fig.2A-D). To investigate whether the pattern we observed in the chicken holds true for other amniotes, we investigated innervation and marker gene expression at the corresponding stage in the mouse embryo (Fig. 2E-G). To test whether there is a long-term relationship between *En1*

expression and epaxial muscle, we lineage-traced *En1*-expressing cells in the new born mouse (Fig.3).

Our analysis shows that the growth cones of the ventral ramus approach the chicken flank myotomes at day 3/ HH20 (Fig.1A,B, arrowheads) and explore the hypaxial environment at day 4/ HH24 (Fig.1C,D, arrowheads). At day 5/HH27, the cutaneous branch of the ventral ramus had penetrated the myotome, projecting towards the surface, then taking a sharp ventrolateral turn (Fig.1E,F, arrowheads). The dorsal ramus lagged behind in its development, being barely visible at stage HH24 but projecting into the epaxial myotome at HH27 (Fig. 1C-F, dr). At embryonic day 4.5/HH25 when both the dorsal and ventral rami contact the myotome, *Myf5* expression was continuous, indicating that the physical separation of epaxial-hypaxial muscle had yet to occur (Fig.2A). *Pax7* expression labelled the dispersing dermomyotome as well as the myotome, in line with the influx of embryonic muscle stem cells into the myotome (Gros et al., 2004; Fig.1B, m; Kahane et al., 2001). Notably, *Pax7* expression was also dorsoventrally continuous. *En1* expression overlapped with the expression of *Pax7* in both the dermomyotome and myotome, in line with the observation that *En1* expression is established in the myotome by the ingressing cells from the dermomyotome (Ahmed et al., 2006; Cheng et al., 2004). Also in line with previous observations, *En1* expression encompassed the dorsal, expaxial part of the myotome and dermomyotome only, forming an expression boundary with the hypaxial marker *Sim1* (Fig.2C,D). Importantly, the dorsal ramus of the spinal nerve projected straight towards the *En1* expression domain (Fig.2C, dr). In contrast, the ventral ramus came close, but by-passed the *En1* domain, with the cutaneous branch projecting into the *Sim1* expression domain at the *En1* boundary and then sharply deflecting away from the *En1* domain (Fig. 2C,D, vr and arrows) and the remainder of the ventral ramus projecting towards the ventrolateral lip of the dermomyotome (Fig. 2C,D, vll).

Somite and skeletal muscle development in the mouse closely resembles that of birds (reviewed by Bryson-Richardson and Currie, 2008; Buckingham, 2006). Yet studies on somitic gene expression had suggested that *En1* and *Sim1* domains overlap rather than abut in the central territory of the mouse dermomyotome (Spörle, 2001). Investigating gene expression at mouse stages that correspond to stages HH20-27 in chicken, we found that mouse expression patterns mirrored that of the chicken, with *En1* labelling the epaxial and *Sim1* the hypaxial dermomyotome at E10.5 (not shown), and *En1* labelling the epaxial myotome at E11.5 (compare Fig.2E,F,G). At later stages when the somite and lateral mesoderm derived dermis precursors merge to form a continuous dermis, *En1* and *Sim1* expression domains extended towards each other and eventually overlapped, both in the chicken and in the mouse (not shown). Using an En1-Cre driver line to express lacZ in all cells that at some

point in development expressed *En1*, we found that in newborn mice, somite- as well as lateral mesoderm-derived dermis had a history of *En1* expression (Fig.3B, dermis). However, the epaxial deep muscles of the back (Fig.3, back muscles) but not the hypaxial panniculus carnosus, psoas, transversus abdominis, external and internal oblique muscles (Fig.3; pc, pm, ta, eo, io, respectively) had expressed *En1* during development. This reconciles the conflicting interpretations and indicates that both mouse and chicken *En1* genes are associated with epaxial myogenesis.

When simultaneously tracing gene expression and axonal projections, we found that in the mouse, the dorsal ramus of the spinal nerve also innervated the *En1* expression domain, while the cutaneous branch of the ventral ramus projected along the border of the *En1* domain and then ventrally away from this; the remainder of the ventral ramus projected towards the ventrolateral extreme of the developing muscle (Fig.2E-G). Thus, in both the chicken and the mouse model, the spinal axons showed the same projections, with the dorsal ramus projecting towards the *En1* domain and the ventral ramus navigating along its border and then ventrolaterally away from it. Like in the chicken, innervation in the mouse occurred when the myotome was still morphologically continuous (Fig.2E,F).

2. Gain- and loss-of-function experiments for amniote *En1*

2.1. Role of *En1* for epaxial-hypaxial somite patterning

To test whether *En1* has a function in epaxial-hypaxial somite patterning, we electroporated the hypaxial domain of chicken flank somites at day 2.5/HH15-16 with the pCaβ vector expressing the lineage tracer GFP as control (Alvares et al., 2003; Fig.4A,B; n=9) or with the pCaβ vector expressing both GFP and mouse *En1* (Fig.4C,D; n=26; mouse *En1* was chosen to discriminate endogenous *En1* and transgene expression). In addition, we targeted epaxial and central territories with the pCaβ control (Fig.4E,F; n=4), with a mixture of pCaβ and the established *En1* siRNA knockdown construct No 150 (Katahira and Nakamura, 2003) (Fig.4G,H; n=8; for control electroporations confirming simultaneous uptake of constructs and activity of siRNA constructs, see Supplementary Material 1) or with a pCaβ construct expressing a dominant-negative from of mouse *En1* in which the EH1 transrepression domain was replaced with the VP16 transactivating domain (Fig.4I,J; n=14). Embryos were incubated overnight to reach HH18-20 and then analysed for the expression of endogenous *En1* using a 3'UTR probe or for the expression of *Sim1*; these probes were tested on mouse embryos and do not hybridise with mouse transcripts (not shown). In all pCaβ-control embryos, the expression domains of *En1* and *Sim1* resembled those of untreated wildtype embryos (Fig.4A,B,E,F, ii-iii, arrows). When mouse *En1* was misexpressed, endogenous *En1* was upregulated (Fig.4Cii,iii, arrowheads) and *Sim1* was downregulated (Fig.4Dii,iii, open arrowheads). When *En1* was knocked down or when the dominant-negative construct was used, endogenous *En1* was

downregulated (Fig.4Gii,iii, open arrowheads) and *Sim1* was upregulated (Fig.4Hii,iii, open arrowheads). This suggests that in the context of somite patterning, *En1* acts as a transcriptional repressor, promoting epaxial and suppressing hypaxial programmes.

2.2. Role of *En1* for dermomyotome and muscle development

Amniote hypaxial myogenesis follows two principle programmes (reviewed by (Wotton et al., 2015)). At flank levels, first the ventrolateral lip (vll) of the dermomyotome, then the adjacent rostrocaudal lips and then the dermomyotome proper contribute cells to the myotome, thereby driving its ventrolateral outgrowth into the body wall. Importantly, these cells stay with the myotome at all times. In contrast, at limb levels, the ventrolateral lips of the dermomyotomes disperse, releasing cells that leave the somite and actively migrate into the limbs to provide the limb musculature. Since *En1* misexpression led to the suppression of hypaxial *Sim1* expression, we wondered whether any of the programmes for hypaxial myogenesis might be affected. To test this, we misexpressed *En1* hypaxially as before, investigating the expression of vll markers (Fig.5), the organisation of the vll and the contribution of electroporated cells to the myotome (Fig.6), marker gene expression in the vll-derived myotome (Fig.7), marker gene expression associated with the central dermomyotome and the rostrocaudal dermomyotomal lips (Fig.8), and the emigration of migratory muscle precursors into the limbs (Fig.9). Unless stated otherwise, embryos were incubated overnight; routinely, 4-8 specimens were analysed for each construct and marker.

Pax3 is a marker for the dermomyotome, with strongly upregulated expression levels in the dorsomedial and ventrolateral lips of the dermomyotome. *MyoR* (=*Musculin*, *Msc*), *EphA4* and *Lbx1* are vll markers, with *Lbx1* only being expressed in limb-level lips and in migrating muscle precursors (Dietrich et al., 1998; Swartz et al., 2001; von Scheven et al., 2006); reviewed by (Wotton et al., 2015)). These markers were expressed normally in pCaβ control-electroporated embryos (Fig.5A,C,E,G). In embryos misexpressing *En1*, *Pax3* expression levels were downregulated to levels found in the central dermomyotome and expression of *MyoR*, *EphA4* and *Lbx1* was lost (Fig.5B,D,F,H, open arrowheads), suggesting that the *En1*-misexpressing vlls were defective.

Histological examination revealed that pCaβ control-electroporated dermomyotomes had the same, epithelial organisation as wildtype dermomyotomes (Fig.6A,B). In somites targeted with the *En1* construct, epaxial cells, i.e. cells also normally expressing *En1*, remained well integrated in the dermomytome (Fig.6D,F, arrowheads). In contrast, the hypaxial dermomyotomes were disrupted: either the vlls had dispersed (Fig.6C,D), or, when the number of *En1* positive cells was high, the cells formed a large, lip-like cell clump (Fig.6E,F). This inability to integrate is possibly a result of *En1* positive cells attempting to sort from the *En1* negative cells as shown in cell aggregation assays in

vitro (Cheng et al., 2004) and confirms that the *En1* misexpressing vlls are defective. Interestingly, both control cells and *En1* misexpressing cells were able to contribute to the myotome (Fig.6B-F, examples labelled by arrows), suggesting that the myogenic capacity was not compromised.

Myf5, *MyoD* and *R-Cadherin* are genes that are sequentially expressed as cells leave the dorsomedial or ventrolateral dermomyotomal lips and contribute to the myotome. Cells from the rostrocaudal lips also eventually express these genes as they differentiate (Berti et al., 2015). We found normal expression patterns in control-electroporated embryos (Fig.7A,C,E); in *En1*-misexpressing embryos, expression in the myotome underneath the vll was downregulated 24 hours after electroporation (Fig.7B,D,F), indicating that the myogenic activity of the vll was perturbed. Marker gene expression and myotome formation later recovered (see also Fig.10 below).

Pax7 is expressed throughout the dermomyotome, with elevated levels in the centre from which the embryonic muscle stem cells arise, and low levels of expression in the dorsomedial and ventrolateral lips. *Alx4* marks the central dermomyotome (epaxial plus hypaxial aspect) as it is not expressed in these lips. *Follistatin* is a marker that labels the myotome and all four dermomyotomal lips, thus including cells that enter the myotome from the rostrocaudal dermomyotomal borders (Ahmed et al., 2006; Berti et al., 2015). Expression of these markers was again unperturbed in control embryos (Fig.8A,C,E). In *En1*-misexpressing embryos, expression of *Alx4* and elevated expression of *Pax7* had extended into the vll (Fig.8B,D, arrowheads), which lacked *Follistatin* expression (Fig.8F, open arrowheads). However, *Follistatin* was still present in the rostrocaudal lips (Fig.8Fi, arrows). Together, this suggests that in *En1* misexpressing somites, the programmes that deliver myogenic cells from the dermomyotomal centre are intact, possibly accounting for the recovery of muscle gene expression and the rescue of myotome formation.

Finally, to analyse the formation of migratory limb muscle precursors, electroporated cells were traced by means of their GFP expression. In control embryos, cells were emigrating from the vll at forelimb levels 24 hours after treatment and had penetrated deep into the limb bud 48 hours after electroporation (Fig.9A,D). In contrast, En1 misexpressing cells failed to emigrate (Fig.9C,D), reflecting that migratory muscle precursor formation requires an intact vll that expresses *Pax3* and *Lbx1* (Brohmann et al., 2000; Dietrich et al., 1999; Grifone et al., 2005; Gross et al., 2000; Schäfer and Braun, 1999; Tremblay et al., 1998).

2.3. Role of *En1* for epaxial-hypaxial innervation of amniote muscle

We showed in Fig.2 that the dorsal ramus of the spinal nerve targets the *En1* expressing myotome whereas the ventral ramus come close but then bypasses this domain. We thus hypothesised that *En1* might influence the outgrowth of the spinal nerve. To test this, we electroporated somites as

before, analysing for the anatomy of the dorsal and ventral ramus of the spinal nerves at day 4.5 of development. We found that in all embryos, the electroporated cells were able to contribute to muscle, confirming that myogenic capacity was not compromised (Fig.10). In the pCaβ-electoporated control embryos, both aspects of the spinal nerves were well-developed (n=12, Fig.10A). In embryos misexpressing *En1*, the dorsal ramus developed correctly (n=15, Fig.10B, dr, and not shown). However, the ventral ramus appeared defasciculated – a typical sign of axons searching for their targets (reviewed in Holt and Harris, 1998). Moreover, the cutaneous branch of the ventral ramus was absent (Fig.10B, open arrowhead). This observation is in line with the idea that, while neurons are set up intrinsically to innervate specific targets, their axonal projections collapse when the targets are absent (Kablar and Rudnicki, 1999; Sharma et al., 2000; Tosney, 1987). Moreover, it suggests that epaxial En1 repels hypaxial axons, thereby guiding them towards their correct, hypaxial targets.

We expected that the knock down of *En1* would lead to the opposite phenotype, a failure of dorsal ramus development. However, electroporation with the *En1* siRNA construct produced inconclusive results, possibly because construct uptake is never complete and hence some cells still expressed *En1* (not shown). We therefore turned to a genetic system, analysing mouse *En1* loss-of-function mutants (Hanks et al., 1995; Kimmel et al., 2000). In E11.5 wildtype (n=6, Fig.10C,E, movie S1) or heterozogous $En1^{+/-}$ littermates (n=4, not shown) the dorsal and ventral ramus of the spinal nerves was well established. In contrast, $En1^{-/-}$ homozygotes (n=10) only developed the ventral ramus that projected to the hypaxial target. The dorsal ramus fell short of its target, unable to recognise or enter the epaxial myotome and dermomyotome (Fig.10D,F, open arrowheads, movie S2). This suggests that *En1* is required to attract the dorsal ramus to the epaxial domain of the somite.

2.4. Role of *En1* for epaxial-hypaxial innervation of actinopterygian muscle

At the outset of the study, we hypothesised that the establishment of Engrailed function in the developing body musculature was a key step in the development and evolution of 3D-mobility in jawed vertebrates, and the experiments conducted in the two amniote models support this idea. Yet amniotes are sarcopterygians, one of three extant gnathostome lineages. To test whether our idea holds true as a general principal for all modern gnathostomes, and because a chondrichthyan model for studies on gene function is currently not available, we turned to the zebrafish, a teleost fish that belongs to the actinopterygian lineage. In the zebrafish, the somites differentiate into sclerotome, myotome and dermomyotome as in other vertebrates (reviewed in Bryson-Richardson and Currie, 2008). Unlike amniotes, however, the early zebrafish myotome delivers almost exclusively fast-twitch muscle; the first slow-twitch muscles stem from a cell population originally located next to the notochord and outside the somite, the adaxial cells. These cells migrate radially

through the fast-twitch musculature, to form a distinct cell layer of slow-twitch muscle atop the fast-twitch myotome. Yet, a subpopulation of the adaxial cells known as muscle pioneers stays behind. The cells first expand caudally then laterally, thereby subdividing the myotome into an epaxial and hypaxial compartment and setting the stage for subsequent horizontal myoseptum development. Significantly, muscle pioneers express all zebrafish *engrailed* genes except *eng2b*, namely *eng1a*, *1b* and *2a* (Thisse and Thisse, 2005). As the prospective superficial slow muscle cells vacate their position next to the notochord, fast-twitch cells fill the space. They also begin to express *eng* and eventually align with the muscle pioneers (Wolff et al., 2003). Studies on axonal projection patterns have been conducted in the zebrafish (reviewed in Fetcho, 1987; Lewis and Eisen, 2003), but not in relation to the *eng* expressing cells. Thus, we simultaneously traced developing motors neurons and *eng* expression (Fig.11A and not shown). To establish *eng* function, we performed gain- (Fig.11B-D) as well as loss-of-function experiments (Fig.11E-G).

When we traced the developing motor axons with the znp1 antibody (Fig.11A, green) and the *eng* expressing cells, visualising GFP expression driven by the *eng2a* promoter (Fig.11A, red), we found that a read-out for *eng2a* was detectable at 13hpf (Maurya et al., 2011) and not shown), muscle was innervated at 18-24 hpf by the three primary motor neurons per somite, which from 26hpf onwards were accompanied by the more numerous secondary motor neurons, thought to be homologous to motor neurons innervating amniote muscle. The axonal projections of the secondary neurons precisely follow the path laid down by the primaries (reviewed in Fetcho, 1987; Lewis and Eisen, 2003). Primary motor neurons all used the same ventral exit point from the neural tube to send their axons to the *eng* expressing cells (Fig.11A, green staining, +). Notably, they reached the *eng* cells before the horizontal myoseptum was fully established. The axons of the with respect to the somite boundaries caudally located neurons are known to temporarily pause at this site. At the stage analysed here, they had proceeded ventrally to innervate the hypaxial myotome. They constitute the ventral ramus (Fig.11A, green staining, vr). The rostrally located neurons kept their axons close to the muscle pioneers to innervate the superficial slow muscles, constituting the fish-specific medial ramus (Fig.11A, mr). The neurons located in the middle of a segment sent their axons dorsally to innervate the epaxial myotome, thereby forming the dorsal ramus (Fig.11A, dr; they eventually retract their connection to the muscle pioneers). Thus, as in mice and chicken, zebrafish motor axons also show an intimate relationship with the *eng* expression domain in the myotome.

To perform gain-of-function experiments, transgenic fish embryos expressing Gal4 under the control of the α actin promoter (i.e. directing expression to muscle; Maurya et al., 2011) were injected at

the 1-2 cell stage with the Gal4-responsive UAS-tRFP control construct (n=8, Fig.11B), with a bicistronic construct harbouring UAS-tRFP and in addition UAS-zebrafish *eng2a* (n≥6, Fig.11C) or a bicistronic constructs containing UAS-mouse *En1* (n≥6, Fig.11D). At 36hpf, embryos that had taken up the injected construct were identified based on their tRFP-driven red fluorescence; their axonal projections were revealed using the znp1 antibody and compared with those of uninjected embryos (n=9, not shown). We found that both types of control embryos exhibited the same axonal projections to the *eng* expressing cells and subsequently away from them. In contrast, in all types of *eng/En* misexpressing embryos, axonal projections were severely disrupted with axons growing in random directions (Fig.11C,D, arrowheads, movie S4), suggesting that they were attracted by multiple targets.

To perform loss-of-function experiments, we employed a morpholino-knock down approach treating embryos with two different control morpholinos (n=11, Fig.11E and not shown; movie S3), with a cocktail of three morpholinos directed against the splice sites of *eng1a,b,2a* (n≥7, Fig.11F), or with a cocktail of six morpholinos directed against the ATG as well as the splice sites of the three *eng* genes (n≥8, Fig.11G, movie S5). At 36hpf, the embryos were again stained with the znp1 antibody. The control embryos all displayed the normal axonal projections. In contrast, in embryos treated with *eng* morpholinos, axonal outgrowth was severely disrupted, with axons this time struggling to reach the central area of the myotome. Notably, *eng* expressing cells were still present (Fig.11F,G; red staining). This suggests that the axons failed to recognise their target, supporting a role for *eng* in the establishment of epaxial-hypaxial innervation patterns also in the fish.

Discussion

Locomotion of invertebrate chordates as well as agnathan/cyclostome vertebrates is based on side-to-side undulations of the body and tail, which creates a thrust against the resistance of the water. The anatomical basis of this movement pattern are re-iterated muscle blocks on either side of the axial midline. These muscle blocks – myotomes - are the key derivatives of the segmented paraxial mesoderm, the somites (reviewed by Bryson-Richardson and Currie, 2008; Buckingham, 2006).

In the early Silurian about 440 million years ago, a new vertebrate group, the jawed vertebrates (gnathostomes), emerged (Brazeau and Friedman, 2015). The earliest representatives of this group, now extinct, were still jawless. Animals with recognisable jaws were present in the mid-Silurian about 430 million year ago, but only one sub-group of these survived. This sub-group, the crown group gnathostomes, encompasses today's chondrichthyans (sharks and rays) and osteichthyans ("bony" vertebrates), with osteichthyans having subdivided into actinopterygians (ray-finned

animals) and sarcopterygians (lobe-finned/limbed animals including tetrapods) by the late Silurian about 420 million years ago. All crown group gnathostomes have myotomes that are subdivided into distinct, separately innervated epaxial (dorsal) and hypaxial (ventral) units. Since each unit can contract independently, complex three-dimensional movement pattern became possible, possibly contributing to their evolutionary success.

Aim of this study was to obtain insight into the establishment of epaxial-hypaxial muscle formation and innervation by comparatively analysing the underlying mechanism in extant gnathostomes. Unfortunately, a chondrichthyan model that allows studies on gene function is not available. However, actinopterygian and sarcopertygian models are well established. These models have their own peculiar features; for example, adaxial cells outside the somite are a speciality of the widely used actinopterygian model, the zebrafish (reviewed by Bryson-Richardson and Currie, 2008). Yet shared developmental programmes can provide insight into conserved mechanisms that evolved in the last common ancestor.

Here, we studied two sarcopterygian models, chicken and mouse, as well as the zebrafish to identify the common denominators for their epaxial-hyapxial muscle development and innervation, and to trace how this mechanism may have evolved. We found that *Engrailed* genes, encoding a homeodomain transcription factor and short range signalling molecule (Alexandre and Vincent, 2003; Brunet et al., 2005; Jimenez et al., 1997; Joliot et al., 1998; Layalle et al., 2011; Maizel et al., 2002; Tolkunova et al., 1998; Wizenmann et al., 2009) are instrumental for this process (summarised in Fig.12 and expanded in Suppl. Fig.2).

Engrailed expression demarcates the epaxial-hypaxial boundary prior to muscle innervation

During vertebrate evolution, the genome was duplicated twice, followed by another whole genome duplication in the actinopterygian lineage that led to the majority of modern fish, the teleosts, which include the zebrafish. Duplicated genes may retain their original function, but frequently, gene loss, sub- or neo-functionalisation occurs (Dehal and Boore, 2005; Holland et al., 1994; Postlethwait, 2007; Taylor et al., 2001). In the mouse and chicken, of the two *Engrailed* genes that were retained, only *Engrailed1* (*En1*) is expressed during myotome development; in the zebrafish, three of its four *engrailed* genes, *eng1a*, *1b*, *2a* (here communally referred to as *eng*) are expressed when muscle forms (Cheng et al., 2004; Devoto et al., 1996; Ekker et al., 1992; Hatta et al., 1991; Spörle, 2001; Thisse and Thisse, 2005).

It is well-established that in zebrafish, *eng* expression commences in the “muscle pioneer cells”, a subpopulation of the so-called adaxial cells that are initially located medial to the myotome, at 13hpf (Ekker et al., 1992; Hatta et al., 1991). The muscle pioneers invade the myotome and settle in a horizontal plane that demarcates the future epaxial-hypaxial divide; they are accompanied by a second *eng* expressing cell population recruited from the medial wall of the myotome proper (Wolff et al., 2003). Thereafter, innervation occurs, with all motor axons initially projecting along the *eng* expressing cells and seeking the muscle pioneers. Subsequently, the axons of the medial ramus remain with the *eng* cells, the ventral ramus deflects ventrally and the axons of the dorsal ramus deflect dorsally (Beattie and Eisen, 1997), reviewed by (Lewis and Eisen, 2003); this study). In mouse and chicken, *En1* expression is established in the myotome by the embryonic muscle stem cells ingressing from the dermomyotome. Expression occupies the epaxial part of the myotome, forming a boundary with the expression domain of the hypaxial marker *Sim1* (Ahmed et al., 2006; Cheng et al., 2004). Expression later spreads in the developing dermis, yet our lineage tracing experiments revealed that the deep muscle of the back (epaxials) but not the hypaxial abdominal muscles have a history of *En1* expression (this study). Upon onset of *En1* expression in the myotome, the motor axons of the spinal nerve approach the myotome, with the hypaxial ramus first projecting towards the *En1* domain, then navigating along its ventrolateral border and penetrating the *En1*-negative hypaxial myotome. Establishment of the dorsal ramus occurs slightly later, with axons targeting the *En1* domain (this study).

Notably, in all models, *En1/eng* expression was established in the myotome before innervation began, and in all models, *En1/eng* expressing cells demarcated the expaxial-hypaxial boundary. Moreover, in all models, axons initially projected towards the *En1/eng* domain, suggesting that in all, the *En1/eng* domain serves as an intermediate target (choice point). Yet in contrast to the zebrafish, in mouse and chicken, the ventral ramus was not allowed entry into the *En1* domain. Anatomical studies suggested that the innervation pattern of epaxial-hypaxial muscle is similar between chondrichthyans and the actinopterygian lineage of bony vertebrates (reviewed in (Fetcho, 1987), suggesting that this pattern reflects the ancestral condition whereas the pattern seen in mouse and chicken is derived. Molecular studies in the zebrafish showed that once axons reached the *eng* expressing cells, their ability to respond to the axonal repellent sema3aa changes, allowing the ventral ramus to project into the hypaxial myotome (Sato-Maeda et al., 2006). It is conceivable that in amniotes, a simple heterochronic change that initiated the deflection of the ventral ramus before the *Engrailed* cells were reached shifted the innervation patterns from the actinopterygian type to the mouse/chicken type (Fig.12).

Avian *En1* is sufficient to promote epaxial and suppress hypaxial somitic programmes

Gain-of-function experiments in the chicken revealed that *En1*, in a cell-autonomous fashion, promotes epaxial marker gene expression and suppresses hypaxial markers, including markers for the lateral dermomyotomal lips. At limb levels, these lips produce migratory muscle precursors that deliver the limb musculature (reviewed by Wotton et al., 2015); upon *En1* misexpression, limb muscle formation was compromised. At flank levels, the lateral lips are important for the outgrowth of hypaxial muscle; however, cells from the rostrocaudal lips and the dermomyotomal centre also contribute (reviewed by Wotton et al., 2015). Here, *En1* misexpression delayed hypaxial myotome development, but eventually, muscle formation recovered. When *En1* was introduced into the hypaxial part of the somite, the misexpressing cells clumped together, thereby disrupting the integrity of the dermomyotomal lips. This is likely a result of the "epaxialised" *En1*-positive cells attempting to sort from the *En1*-negative cells as previously seen in cell aggregation assays (Cheng et al., 2004). However, these *En1* mis-expressing cells were able to contribute to the myotome, indicating that their myogenic potency was unaltered. Together, this suggested that *En1* controls epaxial-hypaxial somite patterning and is sufficient to establish epaxial identities. Interestingly, when *En1* function was knocked down in the chicken, ectopic expression of the hypaxial marker *Sim1* was induced. However, loss of *En1* function in the mouse did not lead to a significant spread of *Sim1* expression. This suggests that other factors contribute to the control of epaxial-hypaxial patterning and can compensate for the loss of the gene. In the zebrafish, both in gain- and in loss-of function experiments, gross morphology of the somite was unaltered, possibly because the ability of the cells to differentiate into muscle was not perturbed.

In all models, *En1/eng* controls the epaxial-hypaxial innervation of muscle

Since in all model organisms, despite their divergent somite organisation, spinal nerves had an intricate relationship with the *En1/eng* expressing cells at the epaxial/hypaxial boundary, we manipulated *En1/eng* function and analysed innervation phenotypes. In the amniote models, when *En1* was misexpressed, the ventral ramus of the spinal nerve defasciculated, axons failed to enter the myotome and the cutaneous branch of the ventral ramus was reduced or absent. When *En1* was knocked out, we observed the phenotype complementary to the gain-of-function experiments: the dorsal ramus of the spinal nerve was retarded. This suggests a role for *En1* in axon guidance at epaxial/hypaxial decision point. In the zebrafish, gain of *eng* function led to aberrant axon growth, as *eng* expressing target cells were now present throughout the myotome. This phenotype was observed both when misexpressing mouse and zebrafish *En1/eng* genes. When *eng* function was knocked down, axonal outgrowth stalled as the cells at the epaxial-hypaxial boundary could not be

identified. These experiments demonstrated that there is an evolutionarily conserved role of *En1/eng* in organising epaxial-hypaxial innervation.

In chicken and mouse, of the two *Engrailed* paralogues, only *En1* is expressed in the somite. In contrast, in the zebrafish all *engrailed* genes with the exception of *eng2b* are expressed in muscle pioneers and associated medial fast muscle cells. Notably, expression of *engrailed* genes at the epaxial-hypaxial boundary has also been described for the dogfish, a chondrichthyan (Tanaka et al., 2002). This suggests that prior to the two (three in teleosts) rounds of vertebrate genome duplication and subsequent gene loss, neo- and sub-functionalisation, the ancestral *eng* gene already had a role in this process. Thus, we can conclude that *Engrailed* facilitated the establishment of segregated, separately innervated epaxial-hypaxial gnathostome muscle and hence, the evolution of gnathostome three-dimensional mobility.

A possible mechanism of *En1/eng* action

It has been proposed for amniotes, that EphrinA molecules deflect the dorsal ramus from the dorsal root ganglion and FGF molecules attract it to the myotome, with neurons of the ventral ramus lacking FgfR1 and thus being unresponsive; (Gallarda et al., 2008; Masuda et al., 2012; Shirasaki et al., 2006), reviewed by (Bonanomi and Pfaff, 2010). Notably, our *En1* gain- and loss-of-function mutations produced phenotypes distinct from that of *FgfR1* loss-and gain-of-function mutants. In the zebrafish, local cues in the extracellular matrix have been proposed to facilitate the organised exit of motor neurons from the spinal cord (Hilario et al., 2010; Schneider and Granato, 2006); reviewed in (Lewis and Eisen, 2003). Yet, while all axons then use the common route to the site of *eng* expression, loss of *eng* expression produced much stronger phenotypes than the genetic or physical ablation of muscle pioneers (reviewed by Lewis and Eisen, 2003). This suggests that in extant vertebrates, *En1/eng* acts in a complex system of guidance cues, with each turn of axons at a choice point being closely regulated. Notably, in the zebrafish, the distance from the motor axon exit point to the *eng* expressing cells is short. In mouse and chicken, the *En1* domain is also close to the ventral root of the spinal cord. Moreover, in our loss-of-function experiments, the ventral ramus was not re-routed; in the gain-of-function experiment, the dorsal ramus was not re-routed. This suggests that while other guidance cues may be long-range, *En1/eng* rather organises short-range axon guidance.

Engrailed proteins are well known for their cell-autonomous function as transcriptional repressors (Jimenez et al., 1997; Tolkunova et al., 1998) and in specific situations, as transcriptional activators (Alexandre and Vincent, 2003). Engrailed may hence act to control the transcription of axon guidance molecules. In the zebrafish, sema3aa is found in the epaxial and hypaxial myotome but not

in the centre, and sema3aa misexpression produces similar phenotypes as loss of *eng* (Halloran et al., 2000), this study). It is possible that here, *eng* transcriptionally suppresses *sema3aa* expression. Yet the phenotype of *En1/eng* misexpression is unaccounted for. Notably, when we investigated the expression patterns of axon guidance molecules in the chicken including Fgf8, Netrin1,2; Rgma,b; Sema3a,c,d,f; EphA4, A7, EphrinA2, A5, A6, and Slit1,2; none was found to be expressed in an *En1*-like pattern. Moreover, for none of them expression patterns were altered upon *En1* misexpression (not shown). Yet Engrailed does not only act as a transcription factor: a number of studies have shown that the Engrailed protein can be secreted (Joliot et al., 1998; Maizel et al., 2002) and can act non-autonomously as a short-range signalling molecule and axon guidance molecule both in vertebrates (Brunet et al., 2005; Wizenmann et al., 2009) and in invertebrates (Layalle et al., 2011). Therefore, it is possible that the main role of *Engrailed* in spinal nerve axon guidance is cell non-autonomous, serving as a secreted signalling molecule. This is supported by the observation that in zebrafish, misexpression of mouse *En1*-VP16 produced phenotypes similar to *En1/eng* misexpression, and that in the chicken, epaxial misexpression of En1-VP16 did not prevent dorsal ramus formation (data not shown) – in both cases, the chimeric molecule can still be exported like wildtype *En1/eng*.

A possible scenario for the evolution of vertebrate 3D-mobility

Fossils only provide limited insight into the organisation of soft tissues, and, perhaps not surprisingly, the existence of a horizontal myoseptum in stem group gnathostomes (i.e. all gnathostome subgroups minus the crown group) is unclear (Trinajstic et al., 2007). In the sister group to gnathostomes, agnathan/cyclostome vertebrates such as the lamprey, myotomes remain dorsoventrally continuous throughout life, and no horizontal myoseptum forms (reviewed in (Fetcho, 1987). Moreover, it is thought that lampreys lack the distinction between the medial and hypaxial motor column that in gnathostomes contain the motor neurons destined to innervate epaxial or hypaxial targets, respectively. This suggests that epaxial-hypaxial muscle and innervation may have evolved late, namely in the last common ancestor of crown group gnathostomes.

Recent studies showed that the lamprey harbours four *En* genes that were multiplied independently in the agnathan lineage and may have assumed novel roles (Matsuura et al., 2008). Remarkably, one of these genes is initially expressed in the centre of the somite before adopting a more widespread pattern (Hammond et al., 2009). Moreover, albeit dorsoventrally continuous, the lamprey myotome is innervated at two discrete points, with axons arborising in the dorsal or ventro-lateral part only (Fetcho, 1987). Furthermore, physiological studies suggest that the lamprey can independently contract the dorsal and ventral aspect of each myotome (Wallen et al., 1985). Given that in our study, the manipulation of *Engrailed* function first and foremost affected axon guidance, it is

possible that with the establishment of centralised *Engrailed* expression, the first steps towards separately innervated epaxial-hypaxial muscles may have been taken before the split of agnathan and gnathostome vertebrates. It cannot be excluded, however, that this central *Engrailed* expression is a result of parallel evolution in the two vertebrate taxa.

Crown group gnathostomes achieved the complete segregation of epaxial-hypaxial muscle, and further studies are needed to establish how the connective tissue of the horizontal myoseptum / thoracacolumbar fascia is being deployed. Yet it is tempting to speculate that, once full three-dimensional mobility was achieved, the way was paved for tetrapods to conquer land: not only had they limbs for locomotion, they also had the core epaxial-hypaxial body muscles to keep their bodies off the ground. When the ancestors of dolphins and whales returned to the water, however, they again had to adapt to swimming through a rather viscous medium. This once more favoured a hydrodynamically optimised body driven by undulating movements. This time, however, evolution took place in a different context: the ancestors of dolphins and whales had a well-developed epaxial-hypaxial musculature. Hence, these animals adapted to their environment, propelling their body forward by upwards-downwards sweeping of the tail as displayed by all cetaceans to date.

Acknowledgements

We are most grateful to L. Alvares, M. Buckingham, J. Clack, P. Currie, L. Erskine, A. Graham, G. Kardon, S. Kuratani, M. Meredith-Smith, A. Prochiantz and S. Roy for inspiring discussions and critical comments to the manuscript, to H. Nakamura for the En siRNA knock down constructs, to Gail Martin for the $En1^{cre/+}$ mouse line and to Hagen Schmidt and Samantha Martin for mouse husbandry. The work was supported by the Human Frontier Science Program, Grant No R6Y0056/2004-C201, the European Network of Excellence Myores, Grant No EU LSHG-CT-2004-511978 MYORES, the Association Françaisecontre les Myopathies, Grant No 11378, the Wellcome Trust, Grant No. WT080470, the Medical Research Council, Grant No. G0601104 and funding from A*STAR.

References

Ahmed, M. U., Cheng, L. and Dietrich, S. (2006). Establishment of the epaxial-hypaxial boundary in the avian myotome. *Dev Dyn* **235**, 1884-1894.

Alexandre, C. and Vincent, J. P. (2003). Requirements for transcriptional repression and activation by Engrailed in Drosophila embryos. *Development* **130**, 729-739.

Alvares, L. E., Schubert, F. R., Thorpe, C., Mootoosamy, R. C., Cheng, L., Parkyn, G., Lumsden, A. and Dietrich, S. (2003). Intrinsic, Hox-dependent cues determine the fate of skeletal muscle precursors. *Dev Cell* **5**, 379-390.

Appel, B., Korzh, V., Glasgow, E., Thor, S., Edlund, T., Dawid, I. B. and Eisen, J. S. (1995). Motoneuron fate specification revealed by patterned LIM homeobox gene expression in embryonic zebrafish. *Development* **121**, 4117-4125.

Beaster-Jones, L., Kaltenbach, S. L., Koop, D., Yuan, S., Chastain, R. and Holland, L. Z. (2008). Expression of somite segmentation genes in amphioxus: a clock without a wavefront? *Dev Genes Evol* **218**, 599-611.

Beattie, C. E. and Eisen, J. S. (1997). Notochord alters the permissiveness of myotome for pathfinding by an identified motoneuron in embryonic zebrafish. *Development* **124**, 713-720.

Berti, F., Meireles Nogueira, J., Wohrle, S., Sobreira, D. R., Hawrot, K. and Dietrich, S. (2015). Time course and side-by-side analysis of mesodermal, pre-myogenic, myogenic and differentiated cell markers in the chicken model for skeletal muscle formation. *J Anat* **227**, 361-382.

Bonanomi, D. and Pfaff, S. L. (2010). Motor axon pathfinding. *Cold Spring Harbor perspectives in biology* **2**, a001735.

Brazeau, M. D. and Friedman, M. (2015). The origin and early phylogenetic history of jawed vertebrates. *Nature* **520**, 490-497.

Brohmann, H., Jagla, K. and Birchmeier, C. (2000). The role of Lbx1 in migration of muscle precursor cells. *Development* **127**, 437-445.

Brunet, I., Weinl, C., Piper, M., Trembleau, A., Volovitch, M., Harris, W., Prochiantz, A. and Holt, C. (2005). The transcription factor Engrailed-2 guides retinal axons. *Nature* **438**, 94-98.

Bryson-Richardson, R. J. and Currie, P. D. (2008). The genetics of vertebrate myogenesis. *Nat Rev Genet* **9**, 632-646.

Buckingham, M. (2006). Myogenic progenitor cells and skeletal myogenesis in vertebrates. *Curr Opin Genet Dev* **16**, 525-532.

Cheng, L., Alvares, L. E., Ahmed, M. U., El-Hanfy, A. S. and Dietrich, S. (2004). The epaxial-hypaxial subdivision of the avian somite. *Dev Biol* **274**, 348-369.

Clack, J. A. (2002). *Gaining Ground. The Origin and Evolution of Tetrapods*. **Bloomington**: *Indiana University Press*.

Currie, P. D. and Ingham, P. W. (1996). Induction of a specific muscle cell type by a hedgehog-like protein in zebrafish. *Nature* **382**, 452-455.

Dehal, P. and Boore, J. L. (2005). Two rounds of whole genome duplication in the ancestral vertebrate. *PLoS Biol* **3**, e314.

Devoto, S. H., Melancon, E., Eisen, J. S. and Westerfield, M. (1996). Identification of separate slow and fast muscle precursor cells in vivo, prior to somite formation. *Development* **122**, 3371-3380.

Dietrich, S. (1999). Regulation of hypaxial muscle development. *Cell Tissue Res* **296**, 175-182.

Dietrich, S., Abou-Rebyeh, F., Brohmann, H., Bladt, F., Sonnenberg-Riethmacher, E., Yamaai, T., Lumsden, A., Brand-Saberi, B. and Birchmeier, C. (1999). The role of SF/HGF and c-Met in the development of skeletal muscle. *Development* **126**, 1621-1629.

Dietrich, S., Schubert, F. R., Healy, C., Sharpe, P. T. and Lumsden, A. (1998). Specification of the hypaxial musculature. *Development* **125**, 2235-2249.

Dolez, M., Nicolas, J. F. and Hirsinger, E. (2011). Laminins, via heparan sulfate proteoglycans, participate in zebrafish myotome morphogenesis by modulating the pattern of Bmp responsiveness. *Development* **138**, 97-106.

Ekker, M., Wegner, J., Akimenko, M. A. and Westerfield, M. (1992). Coordinate embryonic expression of three zebrafish engrailed genes. *Development* **116**, 1001-1010.

Elworthy, S., Hargrave, M., Knight, R., Mebus, K. and Ingham, P. W. (2008). Expression of multiple slow myosin heavy chain genes reveals a diversity of zebrafish slow twitch muscle fibres with differing requirements for Hedgehog and Prdm1 activity. *Development* **135**, 2115-2126.

Ensini, M., Tsuchida, T. N., Belting, H. G. and Jessell, T. M. (1998). The control of rostrocaudal pattern in the developing spinal cord: specification of motor neuron subtype identity is initiated by signals from paraxial mesoderm. *Development* **125**, 969-982.

Fetcho, J. R. (1987). A review of the organization and evolution of motoneurons innervating the axial musculature of vertebrates. *Brain research* **434**, 243-280.

Gallarda, B. W., Bonanomi, D., Muller, D., Brown, A., Alaynick, W. A., Andrews, S. E., Lemke, G., Pfaff, S. L. and Marquardt, T. (2008). Segregation of axial motor and sensory pathways via heterotypic trans-axonal signaling. *Science* **320**, 233-236.

Grifone, R., Demignon, J., Houbron, C., Souil, E., Niro, C., Seller, M. J., Hamard, G. and Maire, P. (2005). Six1 and Six4 homeoproteins are required for Pax3 and Mrf expression during myogenesis in the mouse embryo. *Development* **132**, 2235-2249.

Grimaldi, A., Tettamanti, G., Martin, B. L., Gaffield, W., Pownall, M. E. and Hughes, S. M. (2004). Hedgehog regulation of superficial slow muscle fibres in Xenopus and the evolution of tetrapod trunk myogenesis. *Development* **131**, 3249-3262.

Gros, J., Scaal, M. and Marcelle, C. (2004). A two-step mechanism for myotome formation in chick. *Dev Cell* **6**, 875-882.

Gross, M. K., Moran-Rivard, L., Velasquez, T., Nakatsu, M. N., Jagla, K. and Goulding, M. (2000). Lbx1 is required for muscle precursor migration along a lateral pathway into the limb. *Development* **127**, 413-424.

Halloran, M. C., Sato-Maeda, M., Warren, J. T., Su, F., Lele, Z., Krone, P. H., Kuwada, J. Y. and Shoji, W. (2000). Laser-induced gene expression in specific cells of transgenic zebrafish. *Development* **127**, 1953-1960.

Hamburger, V. and Hamilton, H. L. (1951). A series of normal stages in the development of the chick embryo. *J. Morph.* **88**, 49-92.

Hammond, K. L., Baxendale, S., McCauley, D. W., Ingham, P. W. and Whitfield, T. T. (2009). Expression of patched, prdm1 and engrailed in the lamprey somite reveals conserved responses to Hedgehog signaling. *Evol Dev* **11**, 27-40.

Hanks, M., Wurst, W., Anson-Cartwright, L., Auerbach, A. B. and Joyner, A. L. (1995). Rescue of the En-1 mutant phenotype by replacement of En-1 with En-2. *Science* **269**, 679-682.

Hatta, K., Bremiller, R., Westerfield, M. and Kimmel, C. B. (1991). Diversity of expression of engrailed-like antigens in zebrafish. *Development* **112**, 821-832.

Hilario, J. D., Wang, C. and Beattie, C. E. (2010). Collagen XIXa1 is crucial for motor axon navigation at intermediate targets. *Development* **137**, 4261-4269.

Holland, P. W., Garcia-Fernandez, J., Williams, N. A. and Sidow, A. (1994). Gene duplications and the origins of vertebrate development. *Dev Suppl*, 125-133.

Holt, C. E. and Harris, W. A. (1998). Target selection: invasion, mapping and cell choice. *Curr Opin Neurobiol* **8**, 98-105.

Jimenez, G., Paroush, Z. and Ish-Horowicz, D. (1997). Groucho acts as a corepressor for a subset of negative regulators, including Hairy and Engrailed. *Genes Dev* **11**, 3072-3082.

Joliot, A., Maizel, A., Rosenberg, D., Trembleau, A., Dupas, S., Volovitch, M. and Prochiantz, A. (1998). Identification of a signal sequence necessary for the unconventional secretion of Engrailed homeoprotein. *Curr Biol* **8**, 856-863.

Kablar, B. and Rudnicki, M. A. (1999). Development in the absence of skeletal muscle results in the sequential ablation of motor neurons from the spinal cord to the brain. *Dev Biol* **208**, 93-109.

Kahane, N., Cinnamon, Y., Bachelet, I. and Kalcheim, C. (2001). The third wave of myotome colonization by mitotically competent progenitors: regulating the balance between differentiation and proliferation during muscle development. *Development* **128**, 2187-2198.

Katahira, T. and Nakamura, H. (2003). Gene silencing in chick embryos with a vector-based small interfering RNA system. *Dev Growth Differ* **45**, 361-367.

Kimmel, R. A., Turnbull, D. H., Blanquet, V., Wurst, W., Loomis, C. A. and Joyner, A. L. (2000). Two lineage boundaries coordinate vertebrate apical ectodermal ridge formation. *Genes Dev* **14**, 1377-1389.

Layalle, S., Volovitch, M., Mugat, B., Bonneaud, N., Parmentier, M. L., Prochiantz, A., Joliot, A. and Maschat, F. (2011). Engrailed homeoprotein acts as a signaling molecule in the developing fly. *Development* **138**, 2315-2323.

Lewis, K. E. and Eisen, J. S. (2003). From cells to circuits: development of the zebrafish spinal cord. *Prog Neurobiol* **69**, 419-449.

Logan, C., Hanks, M. C., Noble-Topham, S., Nallainathan, D., Provart, N. J. and Joyner, A. L. (1992). Cloning and sequence comparison of the mouse, human, and chicken engrailed genes reveal potential functional domains and regulatory regions. *Dev Genet* **13**, 345-358.

Maizel, A., Tassetto, M., Filhol, O., Cochet, C., Prochiantz, A. and Joliot, A. (2002). Engrailed homeoprotein secretion is a regulated process. *Development* **129**, 3545-3553.

Martin, B. L. and Harland, R. M. (2001). Hypaxial muscle migration during primary myogenesis in Xenopus laevis. *Dev Biol* **239**, 270-280.

Masuda, T., Sakuma, C., Taniguchi, M., Kanemoto, A., Yoshizawa, M., Satomi, K., Tanaka, H., Takeuchi, K., Ueda, S., Yaginuma, H., et al. (2012). Development of the dorsal ramus of the spinal nerve in the chick embryo: a close relationship between development and expression of guidance cues. *Brain research* **1480**, 30-40.

Matsuura, M., Nishihara, H., Onimaru, K., Kokubo, N., Kuraku, S., Kusakabe, R., Okada, N., Kuratani, S. and Tanaka, M. (2008). Identification of four Engrailed genes in the Japanese lamprey, Lethenteron japonicum. *Dev Dyn* **237**, 1581-1589.

Maurya, A. K., Tan, H., Souren, M., Wang, X., Wittbrodt, J. and Ingham, P. W. (2011). Integration of Hedgehog and BMP signalling by the engrailed2a gene in the zebrafish myotome. *Development* **138**, 755-765.

Mootoosamy, R. C. and Dietrich, S. (2002). Distinct regulatory cascades for head and trunk myogenesis. *Development* **129**, 573-583.

Postlethwait, J. H. (2007). The zebrafish genome in context: ohnologs gone missing. *J Exp Zool B Mol Dev Evol* **308**, 563-577.

Sato-Maeda, M., Tawarayama, H., Obinata, M., Kuwada, J. Y. and Shoji, W. (2006). Sema3a1 guides spinal motor axons in a cell- and stage-specific manner in zebrafish. *Development* **133**, 937-947.

Schäfer, K. and Braun, T. (1999). Early specification of limb muscle precursor cells by the homeobox gene Lbx1h. *Nat Genet* **23**, 213-216.

Schneider, V. A. and Granato, M. (2006). The myotomal diwanka (lh3) glycosyltransferase and type XVIII collagen are critical for motor growth cone migration. *Neuron* **50**, 683-695.

Sharma, K., Leonard, A. E., Lettieri, K. and Pfaff, S. L. (2000). Genetic and epigenetic mechanisms contribute to motor neuron pathfinding. *Nature* **406**, 515-519.

Shirasaki, R., Lewcock, J. W., Lettieri, K. and Pfaff, S. L. (2006). FGF as a target-derived chemoattractant for developing motor axons genetically programmed by the LIM code. *Neuron* **50**, 841-853.

Shirasaki, R. and Pfaff, S. L. (2002). Transcriptional codes and the control of neuronal identity. *Annu Rev Neurosci* **25**, 251-281.

Soriano, P. (1999). Generalized lacZ expression with the ROSA26 Cre reporter strain. *Nat Genet* **21**, 70-71.

Spörle, R. (2001). Epaxial-adaxial-hypaxial regionalisation of the vertebrate somite: evidence for a somitic organiser and a mirror-image duplication. *Dev Genes Evol* **211**, 198-217.

Swartz, M. E., Eberhart, J., Pasquale, E. B. and Krull, C. E. (2001). EphA4/ephrin-A5 interactions in muscle precursor cell migration in the avian forelimb. *Development* **128**, 4669-4680.

Tanaka, M., Munsterberg, A., Anderson, W. G., Prescott, A. R., Hazon, N. and Tickle, C. (2002). Fin development in a cartilaginous fish and the origin of vertebrate limbs. *Nature* **416**, 527-531.

Taylor, J. S., Van de Peer, Y., Braasch, I. and Meyer, A. (2001). Comparative genomics provides evidence for an ancient genome duplication event in fish. *Philos Trans R Soc Lond B Biol Sci* **356**, 1661-1679.

Thisse, B. and Thisse, C. (2005). High Throughput Expression Analysis of ZF-Models Consortium Clones. ZFIN Direct Data Submission.

Tolkunova, E. N., Fujioka, M., Kobayashi, M., Deka, D. and Jaynes, J. B. (1998). Two distinct types of repression domain in engrailed: one interacts with the groucho corepressor and is preferentially active on integrated target genes. *Mol Cell Biol* **18**, 2804-2814.

Tosney, K. W. (1987). Proximal tissues and patterned neurite outgrowth at the lumbosacral level of the chick embryo: deletion of the dermamyotome. *Dev Biol* **122**, 540-558.

Tremblay, P., Dietrich, S., Meriskay, M., Schubert, F. R., Li, Z. and Paulin, D. (1998). A Crucial Role for *Pax3* in the Development of the Hypaxial Musculature and the Long-Range Migration of Muscle Precursors. *Developmental Biology* **203**, 49-61.

Trinajstic, K., Marshall, C., Long, J. and Bifield, K. (2007). Exceptional preservation of nerve and muscle tissues in Late Devonian placoderm fish and their evolutionary implications. *Biology letters* **3**, 197-200.

von Scheven, G., Bothe, I., Ahmed, M. U., Alvares, L. E. and Dietrich, S. (2006). Protein and genomic organisation of vertebrate MyoR and Capsulin genes and their expression during avian development. *Gene Expr Patterns* **6**, 383-393.

Wallen, P., Grillner, S., Feldman, J. L. and Bergelt, S. (1985). Dorsal and ventral myotome motoneurons and their input during fictive locomotion in lamprey. *J Neurosci* **5**, 654-661.

Wizenmann, A., Brunet, I., Lam, J. S., Sonnier, L., Beurdeley, M., Zarbalis, K., Weisenhorn-Vogt, D., Weinl, C., Dwivedy, A., Joliot, A., et al. (2009). Extracellular Engrailed participates in the topographic guidance of retinal axons in vivo. *Neuron* **64**, 355-366.

Wolff, C., Roy, S. and Ingham, P. W. (2003). Multiple muscle cell identities induced by distinct levels and timing of hedgehog activity in the zebrafish embryo. *Curr Biol* **13**, 1169-1181.

Wotton, K. R., Schubert, F. R. and Dietrich, S. (2015). Hypaxial muscle: controversial classification and controversial data? *Results Probl Cell Differ* **56**, 25-48.

Figure Legends

Figure 1. Development of the dorsal and ventral ramus of the avian spinal nerves.

(A,C,E) Lateral views, dorsal to the top, rostral to the right, and (B,D,F) vibratome cross sections, dorsal to the top, medial to the left, of chicken flank somites at 3, 4 and 5 days of development as indicated on the left. Intermediate neurofilaments of nerves were stained using the RMO270 antibody. Growth cones of the ventral ramus contact the developing hypaxial myotome at E3 and begin to enter at E4 (arrowheads). The first axons seeking the epaxial myotome appear at E4. At E5, the cutaneous branch of the ventral ramus has reached the developing dermis and has turned ventrally, the dorsal ramus has reached the epaxial myotome and started to arborise in this territory.

Abbreviations: dr, dorsal ramus; drg, dorsal root ganglion; E3/4/5, day 3/4/5 of development; HH20/24/27, Hamburger and Hamilton stage 20/24/27 of chicken development; sn, spinal nerve; vr, ventral ramus; the asterisk marks the ventral root of the spinal cord.

Figure 2. Epaxial-hypaxial subdivision and innervation of the developing amniote musculature.

(A-D) Cross sections of chicken flank somites at E4.5 of development, dorsal to the top, medial to the left. Somitic gene expression detected by in situ hybridisation is displayed in blue, axons are detected with the RMO 270 antibody in brown. (A) *Myf5* gene expression labels cells in the myotome. (B) *Pax7* expression marks the dermomyotome and embryonic muscle stem cells that leave the centre of the dermomyotome and enter the myotome. (C) A dorsally located subset of the *Pax7* positive cell population expresses *En1*, (D) a ventrally located subset expresses *Sim1*. The *En1-Sim1* expression boundary demarcates the epaxial-hypaxial boundary (dotted line). The ventral ramus of the spinal nerve comes close to the *En1* expression domain, but navigates around it and targets the hypaxial myotome; first contact with the myotome is made when axons of the cutaneous branch of the ventral ramus navigate along the ventral boundary of the *En1* domain and project through the *Sim1* domain towards the dermis (small arrows). Axons of the dorsal ramus (arrowhead) target the *En1* domain. (E-G) Cross sections of mouse flank somites at E11.5 of development, dorsal to the top, medial to the left; somitic gene expression in blue, RMO staining in brown; markers are indicated on top of the corresponding image. Note that marker gene expression and axonal projections in the mouse closely match that of the chicken.

Abbreviations: d, dermis precursors; dm, dermomyotome; dml, dorsomedial lip of the dermomyotome; dr, dorsal ramus of the spinal nerve; drg, dorsal root ganglion; e, epaxial; h, hypaxial; m, myotome; scl, sclerotome; vll, ventrolateral lip of the dermomyotome; vr, ventral ramus of the spinal nerve. The asterisk marks the axons of motor neurons projecting out of the neural tube, arrows indicate axons of the cutaneous branch of the ventral ramus, arrowheads the dorsal ramus.

Figure 3. Epaxial muscles are derived from *En1* expressing cells.

Lumbar region of a newborn *En1-Cre;R26R*^{LacZ} mouse, obtained by crossing an *En1*-Cre heterozygous male with a Rosa26-lacZ female, dorsal to the top. (A) Whole mount lacZ staining (blue) revealing all cells that ever in their development expressed *En1*; skin, ventral body wall and internal organs removed. The epaxial deep back muscles are derived from *En1* expressing cells. Cross section of the lumbar region; (B) skeletal muscle staining for fast muscle Myosin (green), (C) lacZ staining (blue) revealing cells with a history of *En1* expression. There is a wider contribution of *En1* cells to the dermis, yet the epaxial deep back muscles but not the hypaxial abdominal and panniculus carnosus muscles are derived from *En1* cells.

Abbreviations: eo, external oblique muscle; io, internal oblique muscle; na, neural arch; pc, panniculus carnosus muscle; pm, psoas muscle; sc, spinal cord; ta, transversus abdominis muscle; vb, vertebral body. The arrow points at the origin of the abdominal muscles at the thoracolumbar fascia which is also derived from *En1* cells.

Figure 4. Gain and loss of chicken *En1* function changes epaxial-hypaxial marker gene expression.

Lateral views (i,ii; anterior to the top) and cross sections (iii; dorsal to the top, medial to the left) of flank somites, 24 hours after electroporation with (A,B,E,F) a GFP expressing control construct, (C,D) a bicistronic construct expressing GFP and mouse *En1*, (G,H) the GFP control construct together with a chicken *En1* siRNA knockdown construct, (I,J) a bicistronic construct expressing GFP and mouse*En1-V16*. In (A-D), the hypaxial domain, in (E-H) the expaxial and central domains of the somite were targeted; embryos were analysed 24 hours later for the expression of endogenous *En1* and *Sim1* as indicated at the top of the panel. Hypaxial and epaxial control electroporations did not interfere with the expression of *En1* and *Sim1* (A,B,E,F, arrows). However, misexpression of mouse *En1* upregulated endogenous *En1* and downregulated *Sim1* (C,D, arrowheads); knock down of chicken *En1* or misexpression of *En1-Vp16* led to loss of *En1* and upregulation of *Sim1* expression (G,H, open arrowheads).

Figure 5. Hypaxial misexpression of *En1* suppresses markers for the ventrolateral lips of the dermomyotome.

Lateral views and cross sections of (A-F) flank somites and (G,H) forelimb level somites 24 hours after electroporation, displayed as in Fig.4. Markers stained for in blue are indicated on the left; in (F,H), the mRNA of the construct was also visualised (red staining). In embryos electroporated with the control construct, normal expression patterns were observed for all markers, with (A)*Pax3* displaying elevated levels of expression in the ventrolateral lips of the dermomyotome (vll), (C)*MyoR* expression labelling the vll only, (E)*EphA4* labelling the vll and the neighbouring lateral mesoderm, and (G)*Lbx1* expression indicating premigratory and migrating limb muscle precursors. In *En1* misexpressing somites, elevated *Pax3* expression and any somitic expression of *MyoR*, *Epha4* and *Lbx1* was lost (open arrowheads), only the *Epha4* expression in the lateral mesoderm remained.

Figure 6. Hypaxial misexpression of *En1* disrupts the morphology of the ventrolateral lips (vll) of the dermomyotome.

Cross sections stained for the expression of the electroporated constructs (brown staining) and haematoxylin-eosin (purple and red) 24 hours after electroporation, dorsal to the top, medial to the left. In (A) wildtype and (B) control-electroporated somites, the vlls are well-organised epithelial structures. (C-F) In *En1* misexpressing somites, the vlls are either dispersed or the misexpressing cells clump together, providing a lip-like appearance. Where *En1* misexpression encompassed epaxial areas, the epithelial organisation of the dermomyotome remained intact (arrowheads) suggesting that the *En1* misexpressing cells integrate into the *En1* expressing epaxial dermomyotome but sort from *En1* negative hypaxial cells. Note that *En1* misexpressing cells populated the myotome (examples marked by arrows), hence myogenic capacity is not compromised.

Figure 7. Hypaxial misexpression of *En1* hinders myoblast deposition from the vll.

Lateral views and cross sections of flank somites as in Fig.4, the markers stained for are indicated on the left. (A,C,E) In control-electroporated embryos, the myotomal markers *Myf5*, *MyoD* and *R-Cadherin* (*Cadherin4*) label the myotome including cells emerging from the vll. (B,D,F) When *En1* was misexpressed, gaps in the ventrolateral myotomes appeared, judged by the absence of marker gene expression (open arrowheads).

Figure 8. Hypaxial misexpression of *En1* expands the central somitic programmes ventrolaterally.

Lateral views and cross sections of flank somites as in Fig.4, the markers stained for are indicated on the left. (A) In control embryos, *Pax7* expression is strong in the dermomyotome proper, weak in the

lips. (B) In *En1* misexpressing embryos, strong *Pax7* expression encompassed the vll. (C) In control embryos, *Alx4* expression labels the central dermomyotome destined to contribute to the dermis. (D) In *En1* misexpressing embryos, *Alx4* expression extended into the vll. (E) In controls, *Follistatin* was expressed in an irregular pattern along all four dermomyotomal lips and in the myotome. (F) In *En1* misexpressing embryos, *Follistatin* expression in the vll was reduced; the other lips still expressed the gene.

Figure 9. Hypaxial misexpression of *En1* suppresses the formation of migratory muscle precursors

Lateral views of somites at forelimb levels, (A,C) 24 hours and (B,D) 48 hours after electroporation, rostral to the top, medial to the left; the position of the vll is marked. (A,B) In control embryos, the limb muscle precursors migrate into the limb bud. (C,D) In the experimental embryos, the *En1*-misexpressing cells fail to emigrate.

Figure 10. Gain and loss of amniote *En1* function causes complementary innervation phenotypes.

(A, B) Cross sections of chicken somites 48 hours after electroporation with (A) the control or (B) the mouse *En1* construct; orientation and abbreviations as in Fig.2. Targeted cells were detected with a GFP probe (blue), nerves by RMO antibody staining (brown). In both the control and the *En1* misexpressing embryos, electroporated cells populated the myotome. In the control, the ventral ramus of the spinal nerve was well-developed, with the cutaneous branch of the ventral ramus projecting through the myotome towards the developing dermis (A, arrow), as seen for untreated embryos (compare with Fig.2A-D). (B) In contrast, ectopic expression of *En1* caused defasciculation of the ventral ramus and prevented the outgrowth of the cutaneous branch of this ramus (open arrowhead).

(C,D) Lateral views (anterior to the right, dorsal to the top) and (E,F) cross sections (displayed as in A,B) of wildtype (C,E) and *En1*-deficient mice (D,F) at E11.5 of development; the nerves were revealed with the RMO antibody (green staining). In the wildtype, the dorsal ramus of the spinal nerve has reached the epaxial somite (C,E, arrows), in the mutant, the dorsal ramus has fallen short of its target (D,F, open arrowheads).

Figure 11. Gain and loss of zebrafish *eng* function causes complementary innervation phenotypes.

(A) Cross section of a 36hpf zebrafish eng2a:GFP embryo (transgene expression shown in red); axons were stained with the znp1 antibody (green) and cell nuclei with Dapi (blue). Initially, the primary

motor neurons all projected to the *eng* expressing muscle pioneers (mp, strong staining) and the accompanying fast muscle cells (weaker staining), which together subdivide the myotome into an epaxial and hypaxial portion at the position marked by (+) and organise the formation of the horizontal myoseptum. At the stage shown, the secondary motor neurons have also formed. Neurons aligned with the caudal somite half have extended their axons ventrally to form the ventral ramus and innervate the hypaxial myotome. Motor neurons next to the rostral somite half send their axons laterally along the developing horizontal myoseptum to form the medial ramus and target the superficial slow muscles. Motor neurons facing the rostrocaudal centre of each segment project dorsally to form the dorsal ramus and innervate the epaxial myotome; they eventually withdraw their connection to the *eng*+ cells. Abbreviations: dr, dorsal ramus; mp, muscle pioneers; mr, medial ramus; vr, ventral ramus; Dr, *Danio rerio*; Mm, *Mus musculus*.

(B-G) Lateral views of 36hpf control (B,E) and experimental (C,D,F,G) embryos, anterior to the left. The position of the developing horizontal myoseptum is indicated by a stippled line.

(B-D) Gain-of-function experiments: transgenic α actin-Gal4 embryos injected with (B) a UAS-tRFP control construct, (C) a bicistronic UAS- driven construct expressing tRFP and zebrafish *eng2a*, or (D) a bicistronic construct expressing tRFP and mouse *En1* as indicated at the top of the panel. Cells that have taken up the constructs fluoresce in red (anti-tRFP); axons are revealed with the znp1 antibody in green. When *Engrailed* genes were misexpressed throughout the somite, motor axons were severely misguided (C,D, arrowheads).

(E-G) Loss-of-function experiments: eng2a:GFP embryos (transgene expression shown in red, znp1-stained axons in green) treated with (E) a control morpholino, (F) a morpholino cocktail targeting the splice sites of all *eng* genes expressed in the somite, or (G) a morpholino cocktail targeting the *eng1a*,*b*,*2a*ATG and the splice sites. Knock down of *eng* blocked axonal outgrowth, and axons stalled or took up erratic paths in search for their targets (F,G, open arrowheads).

Figure 12. Gnathostome spinal axons and their relationship with the somitic *Engrailed* domain.

In teleosts, all motor axons are attracted by the *Engrailed* domain which serves as temporary target. Subsequently, the dorsal and ventral ramus becomes deflected to innervate the epaxial and hypaxial muscles, respectively, thereby establishing three-dimensional mobility. In amniotes, the dorsal ramus of the spinal nerve is also attracted by the *Engrailed* domain. The ventral ramus approaches the *Engrailed* domain but is deflected ventrolaterally without contacting the *Engrailed* expressing cells. It can be speculated that in amniotes, the mechanism that controls the secondary deflection

from the *Engrailed* cells has been brought forward in time (heterochronic shift). However, in all gnathostomes, *Engrailed* is key to the epaxial-hypaxial innervation of muscle.

Abbreviations: T0: time point when axons contact the *Engrailed* expressing cells. T1: time when axons are deflected away from the Engrailed domain. T-1: time to which the deflection of the amniote ventral ramus may have been brought forward.

Supplementary material

Suppl. Figure 1. Simultaneous uptake of constructs.

Lateral views of chicken flank somites 24 hours after electroporation, rostral to the top, medial to the left. (i) Image depicting red fluorescence only, (ii) green fluorescence and (iii) red and green fluorescence combined. The constructs are indicated on the right of the panel.

(A) Two neighbouring somites were electroporated individually with a construct expressing red fluorescent protein (RFP; No1) or green fluorescent protein (GFP, No2). RFP and GFP expression was confined to the respective somites.

(B) Three somite were electroporated with an equimolar mix of the RFP and GFP expressing constructs. Somites show the same distribution of red and green fluorescence.

(C) Three somite were electroporated with (No1) a bicistronic construct expressing RFP and a siRNA targeting the mRNA for GFP, or (No2) a mix of the RFP-siRNA expressing construct and a construct expressing GFP, or (No3) the GFP expressing construct alone. In No2, almost all green fluorescence was extinguished, indicating that the constructs were taken up into the same cells, thus allowing the siRNA to block GFP protein production.

Suppl. Figure 2. Establishment of the central *Engrailed* expression domain correlates with vertebrate epaxial-hypaxial innervation of muscle and the evolution of three-dimensional mobility.

Compilation of extant chordate body muscle anatomy and innervation, *Engrailed* expression, our experimental data on *Engrailed* function, and chordate phylogeny (showing crown group representatives only). Vertebrate taxa that are established as model organisms are highlighted in yellow.

(*1) In tunicates, segmented body muscle was secondarily reduced during evolution; (*2) in amphibians, hypaxial body muscle is laid down by a derived mechanism that employs migratory muscle precursors (Martin and Harland, 2001). Thus, both taxa represent derived models of body muscle formation.

In lancelets, *engrailed* expression is found in the posterior half of the rostral-most somites, which have properties not shared by the somites in the trunk or vertebrate somites (reviewed in (Beaster-Jones et al., 2008). Expression is not confined to a myotomal subdomain, muscle synapses directly with neurons in the spinal cord (reviewed in (Fetcho, 1987). In agnathans, muscle is dorsoventrally continuous. Yet distinct dorsal and ventral rami of the spinal nerves that can trigger localised dorsal or ventral muscle contraction (Wallen et al., 1985) as well as centralised embryonic *Engrailed* expression are already present (Hammond et al., 2009; Matsuura et al., 2008). In crown group gnathostomes, epaxial-hypaxial muscle segregation and innervation is well established (reviewed in (Fetcho, 1987). Notably, in chondrichthyans (Tanaka et al., 2002), teleosts (Devoto et al., 1996; Ekker et al., 1992; Hatta et al., 1991; Thisse and Thisse, 2005), amphibians (Grimaldi et al., 2004) chicken (Ahmed et al., 2006; Cheng et al., 2004) and mouse (Spörle, 2001), *Engrailed* gene expression is found in a centrally located domain of the myotome. The experimental data shown here indicate a conserved function of *Engrailed* in extant gnathostome epaxial-hypaxial muscle innervation. It is therefore possible that the recruitment of *Engrailed* for the control this distinct innervation pattern occurred before the agnathan-gnathostome split. Full, physical segregation of epaxial-hypaxial muscles, and hence full three-dimensional mobility however was only achieved in the gnathostome lineage.

Movie S1.

Arborisation of the dorsal ramus of E11.5 wildtype mouse spinal nerve at flank levels, stained with the Tuj1 antibody; external view, dorsal to the top, anterior to the right.

Movie S2.

One of the least affected dorsal rami in E11.5 $En1^{-/-}$ mouse mutant, stained with the Tuj1 antibody and viewed as in movie S1. The dorsal ramus is severely underdeveloped; it just about has reached the surface and shows little arborisation.

Movie S3.

3D rotation of 36hpf zebrafish motor axons of the embryo shown in Fig. 11E, treated with the control morpholino; rotation starting with an external view, dorsal to the top, anterior to the left. All motor neurons project to the Engrailed domain, and then away from it.

Movie S4.

3D rotation of 36hpf zebrafish motor axons of the *eng2a* overexpressing embryo in Fig.11C; rotation as in movie S3. Motor axons show random projections, indicating that they fail to recognise a discrete target.

Movie S5.

3D rotation of 36hpf zebrafish motor axons of the embryo in Fig.11G, treated with the cocktail of six *eng* morpholinos; rotation as in movie S3. Motor axons fail to recognise and project towards the muscle pioneers and associated fast cells at the epaxial-hypaxial interface.

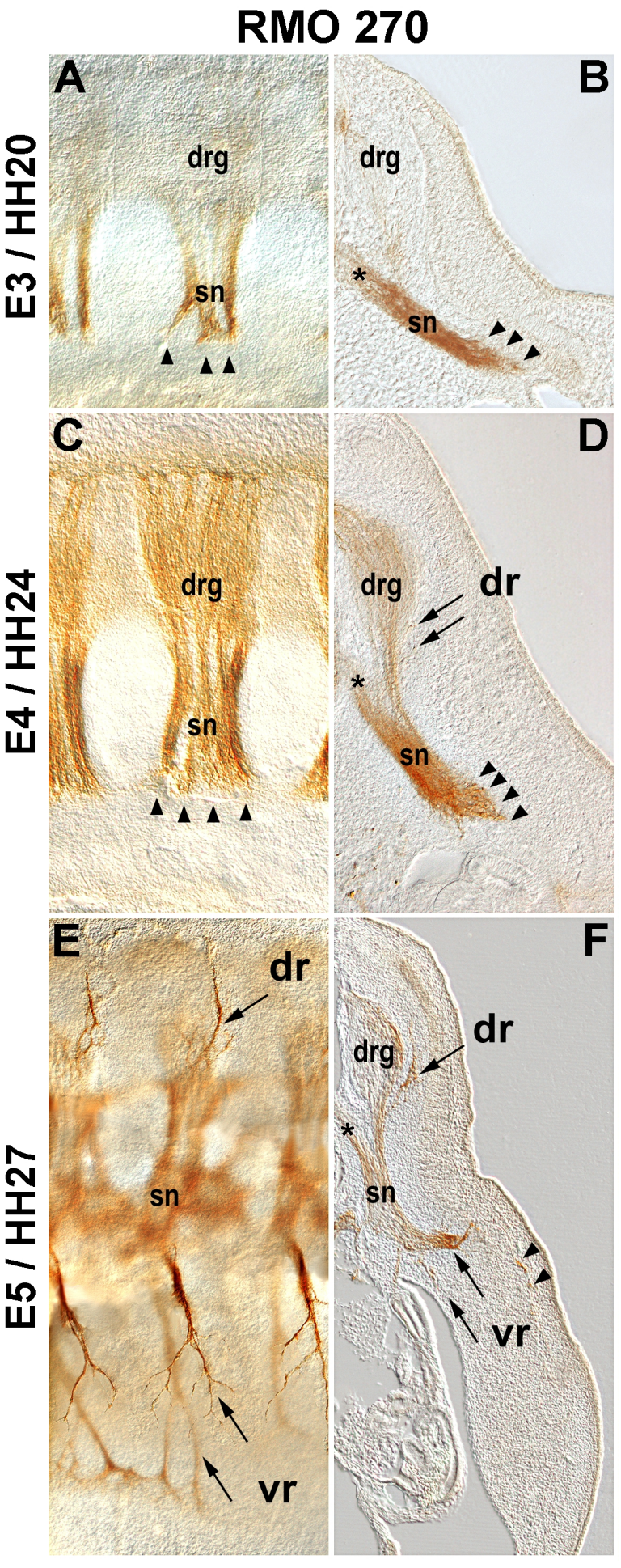
RMO 270
E3 / HH20
E4 / HH24
E5 / HH27
A
B
C
D
E
F
drg
sn
dr
vr
*

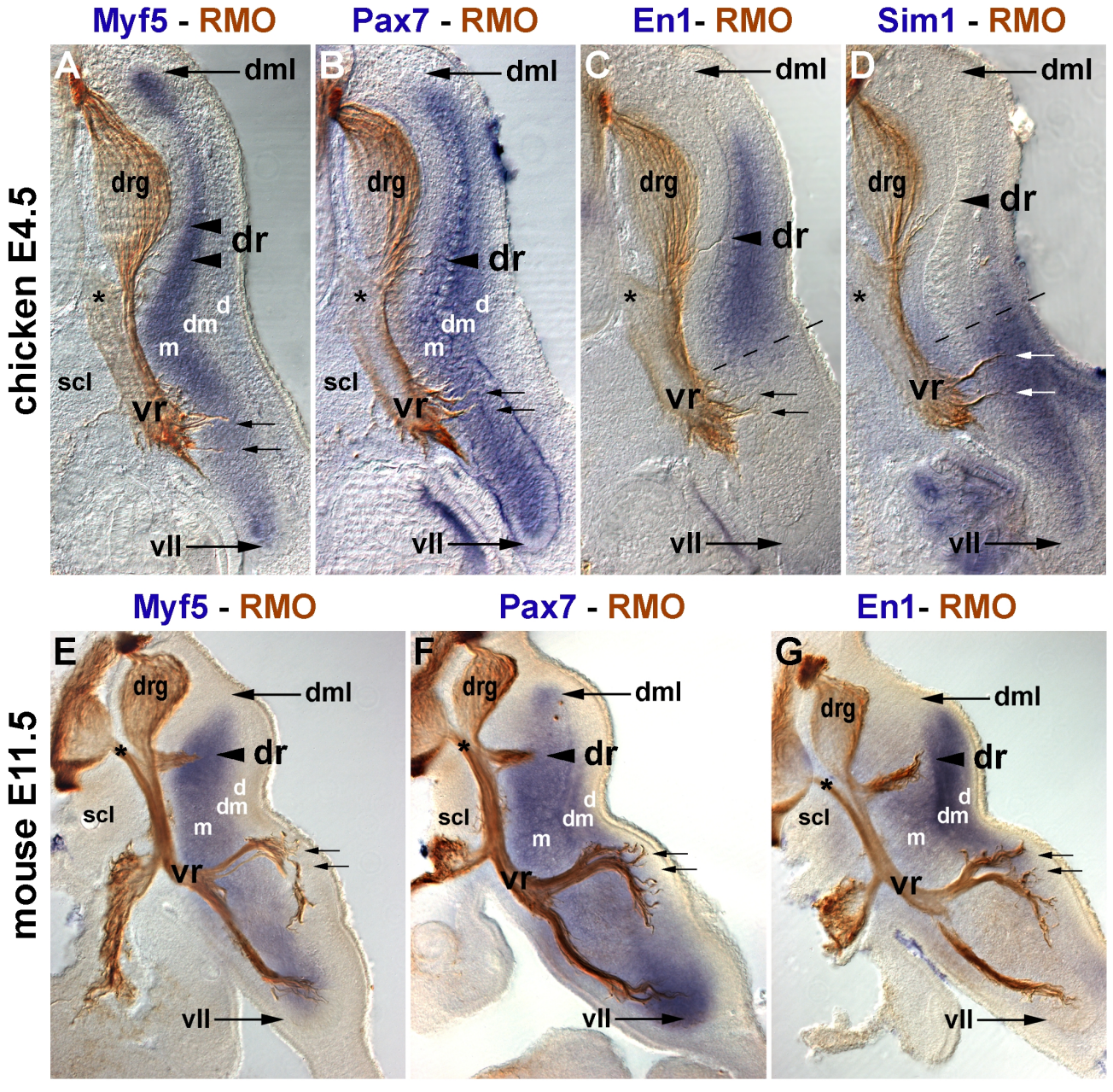
Myf5 - RMO
Pax7 - RMO
En1- RMO
Sim1 - RMO
chicken E4.5
A
B
C
D
dml
drg
dr
d
dm
m
scl
vr
vll
*
Myf5 - RMO
Pax7 - RMO
En1- RMO
mouse E11.5
E
F
G

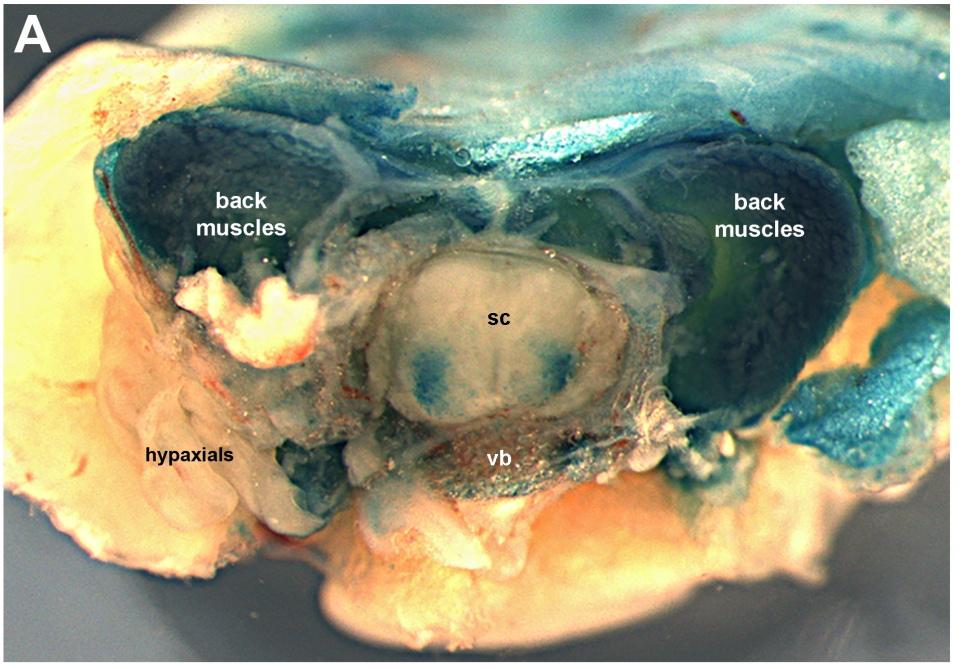
A
back
muscles
back
muscles
sc
hypaxials
vb

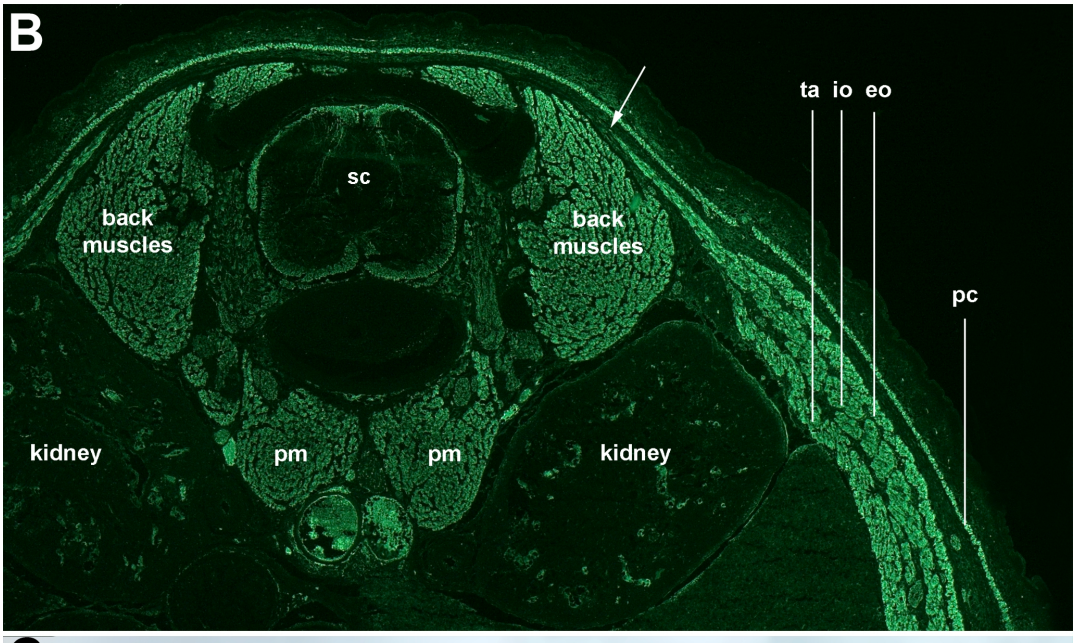
B
ta io eo
sc
back
muscles
back
muscles
pc
kidney
pm
pm
kidney

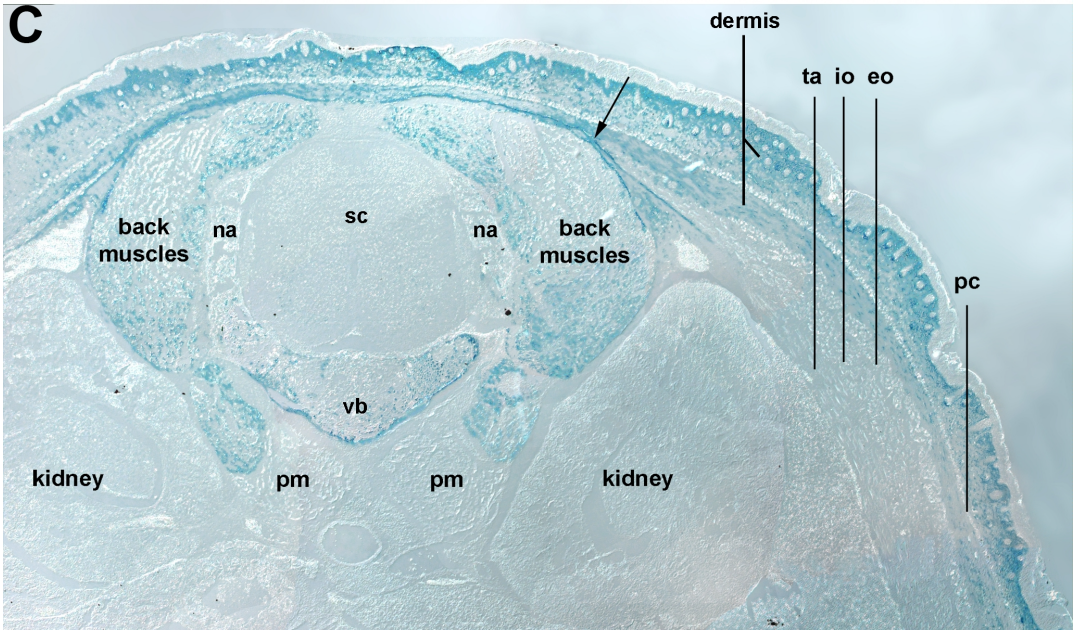
C
dermis
ta io eo
back
muscles
na
sc
na
back
muscles
pc
vb
kidney
pm
pm
kidney

marker: chicken En1
marker: chicken Sim1
hypaxial electroporations
epaxial-central electroporations
pCaβ control
mouse En1
pCaβ control
chicken En1 siRNA
mouse En1-Vp16
Ai
Aii
Aiii
Bi
Bii
Biii
Ci
Cii
Ciii
Di
Dii
Diii
im
Ei
Eii
Eiii
Fi
Fii
Fiii
im
Gi
Gii
Giii
Hi
Hii
Hiii
im
Ii
ii
Iiii
Ji
Jii
Jiii
im

control
mouse En1 misexpression
Pax3
MyoR
EphA4
Lbx1
Ai
Aii
Aiii
Bi
Bii
Biii
Ci
Cii
Ciii
Di
Dii
Diii
Ei
Eii
Eiii
Fi
Fii
Fiii
Gi
Gii
Giii
Hi
Hii
Hiii

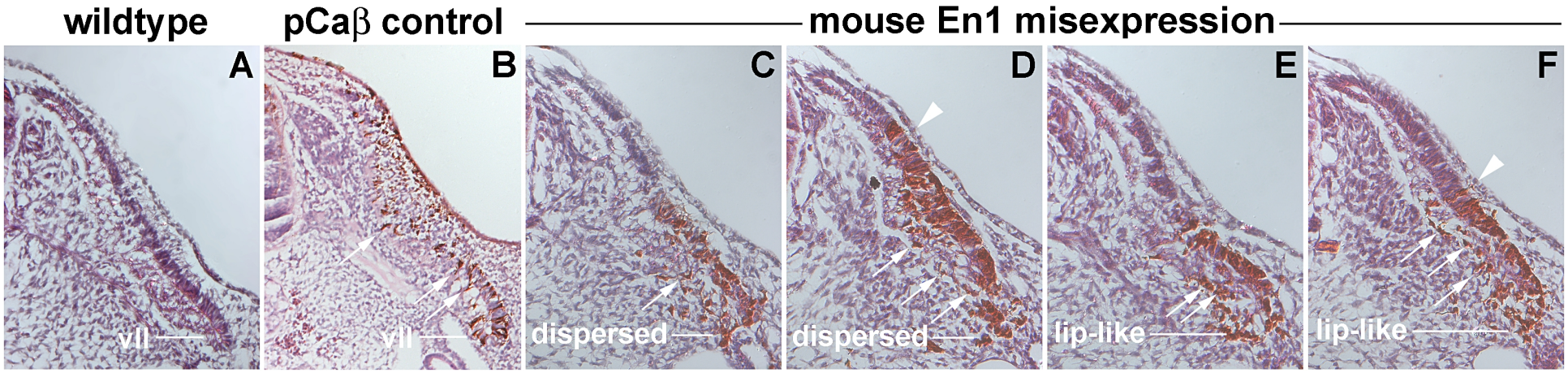
wildtype
pCaβ control
mouse En1 misexpression
A
B
C
D
E
F
vII
vII
dispersed
dispersed
lip-like
lip-like

pCaβ control
mouse En1
Myf5
MyoD
R-Cadherin
Ai
Aii
Aiii
Bi
Bii
Biii
Ci
Cii
Ciii
Di
Dii
Diii
Ei
Eii
Eiii
Fi
Fii
Fiii

pCaβ control
mouse En1
Pax7
Alx4
Follistatin
Ai
Aii
Aiii
Bi
Bii
Biii
Ci
Cii
Ciii
Di
Dii
Diii
E
Ei
F
Fi

24h HH20
48h HH22
pCaβ control
mouse En1
A
B
C
D
vII
vII
vII
vII

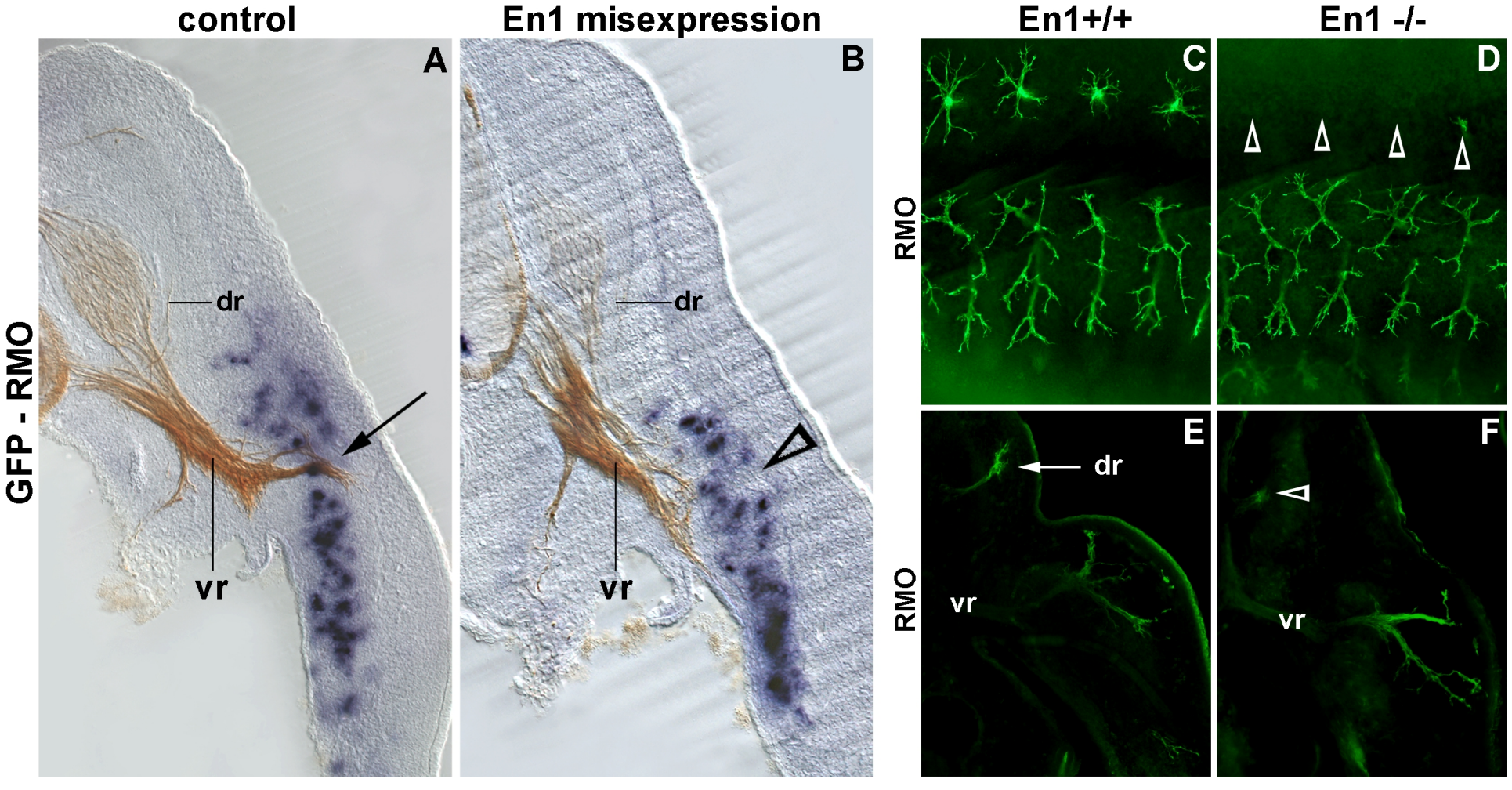
control
En1 misexpression
En1+/+
En1 -/-
GFP - RMO
RMO
RMO
A
B
C
D
E
F
dr
vr
dr
vr
dr
vr
vr

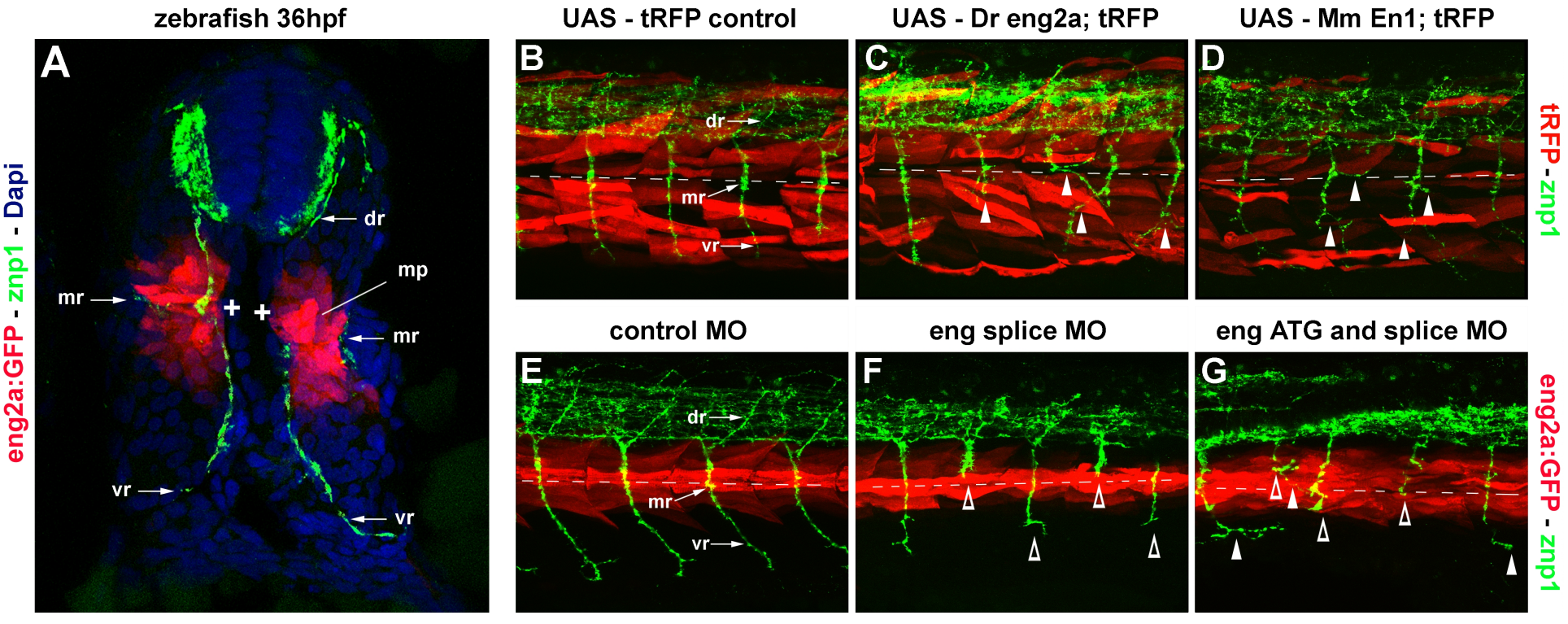
zebrafish 36hpf
UAS - tRFP control
UAS - Dr eng2a; tRFP
UAS - Mm En1; tRFP
A
B
C
D
eng2a:GFP - znp1 - Dapi
tRFP - znp1
dr
mr
mp
vr
control MO
eng splice MO
eng ATG and splice MO
E
F
G
eng2a:GFP - znp1

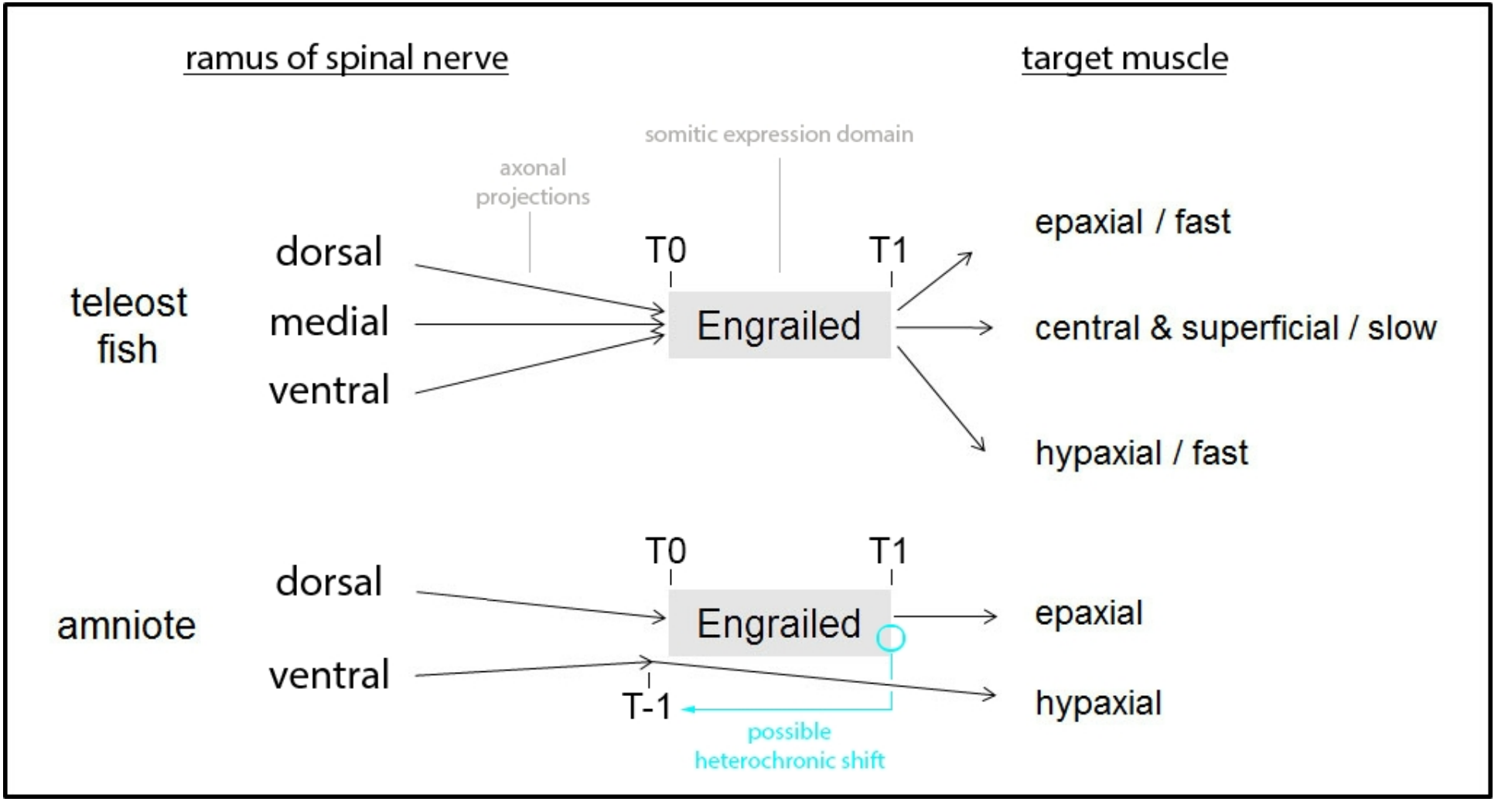
ramus of spinal nerve
target muscle
somitic expression domain
axonal projections
teleost fish
dorsal
medial
ventral
T0
T1
Engrailed
epaxial / fast
central & superficial / slow
hypaxial / fast
amniote
dorsal
ventral
T0
T1
Engrailed
epaxial
hypaxial
T-1
possible heterochronic shift

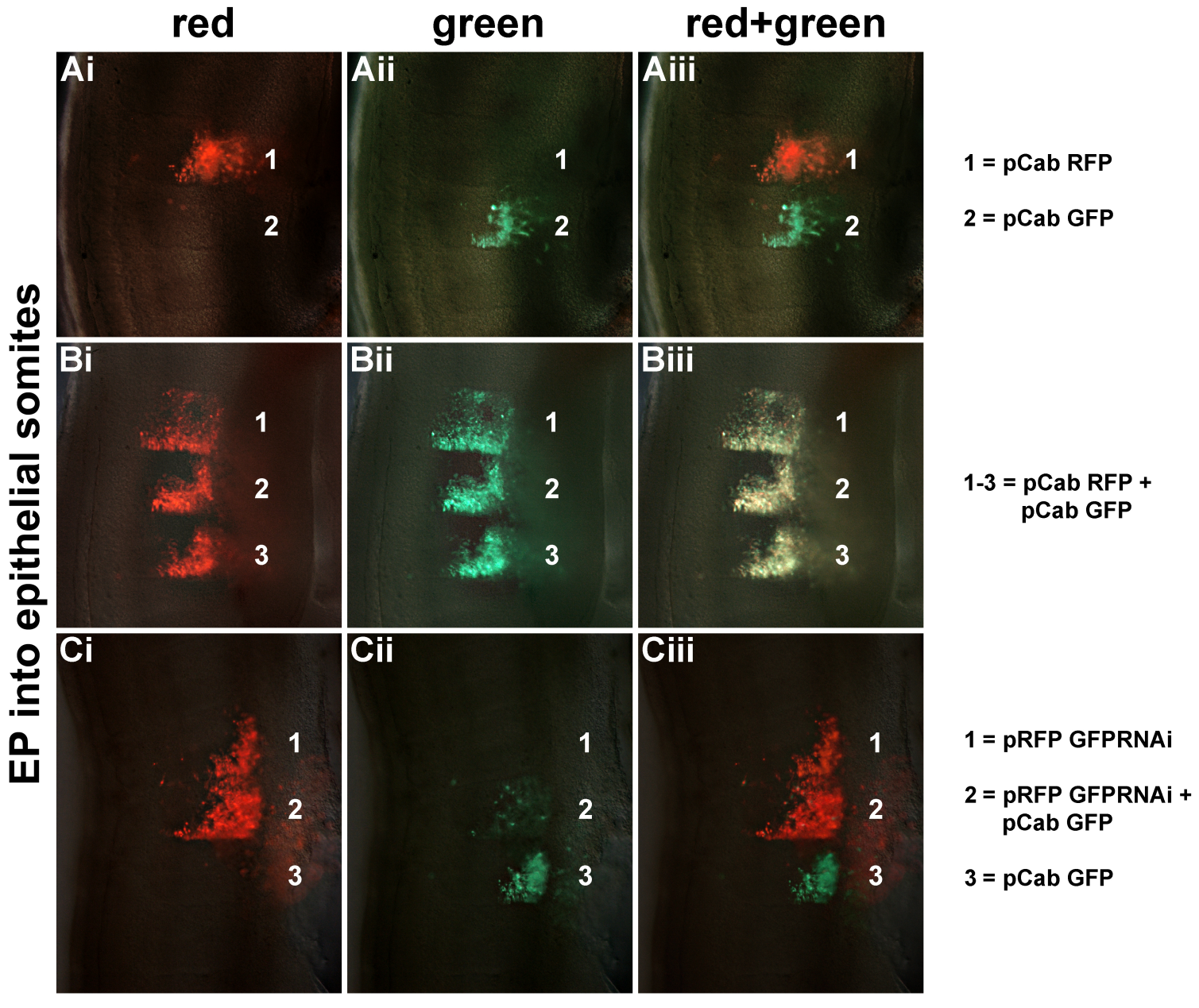
red
green
red+green
EP into epithelial somites
Ai
Aii
Aiii
Bi
Bii
Biii
Ci
Cii
Ciii
1
2
3
1 = pCab RFP
2 = pCab GFP
1-3 = pCab RFP +
pCab GFP
1 = pRFP GFPRNAi
2 = pRFP GFPRNAi +
pCab GFP
3 = pCab GFP

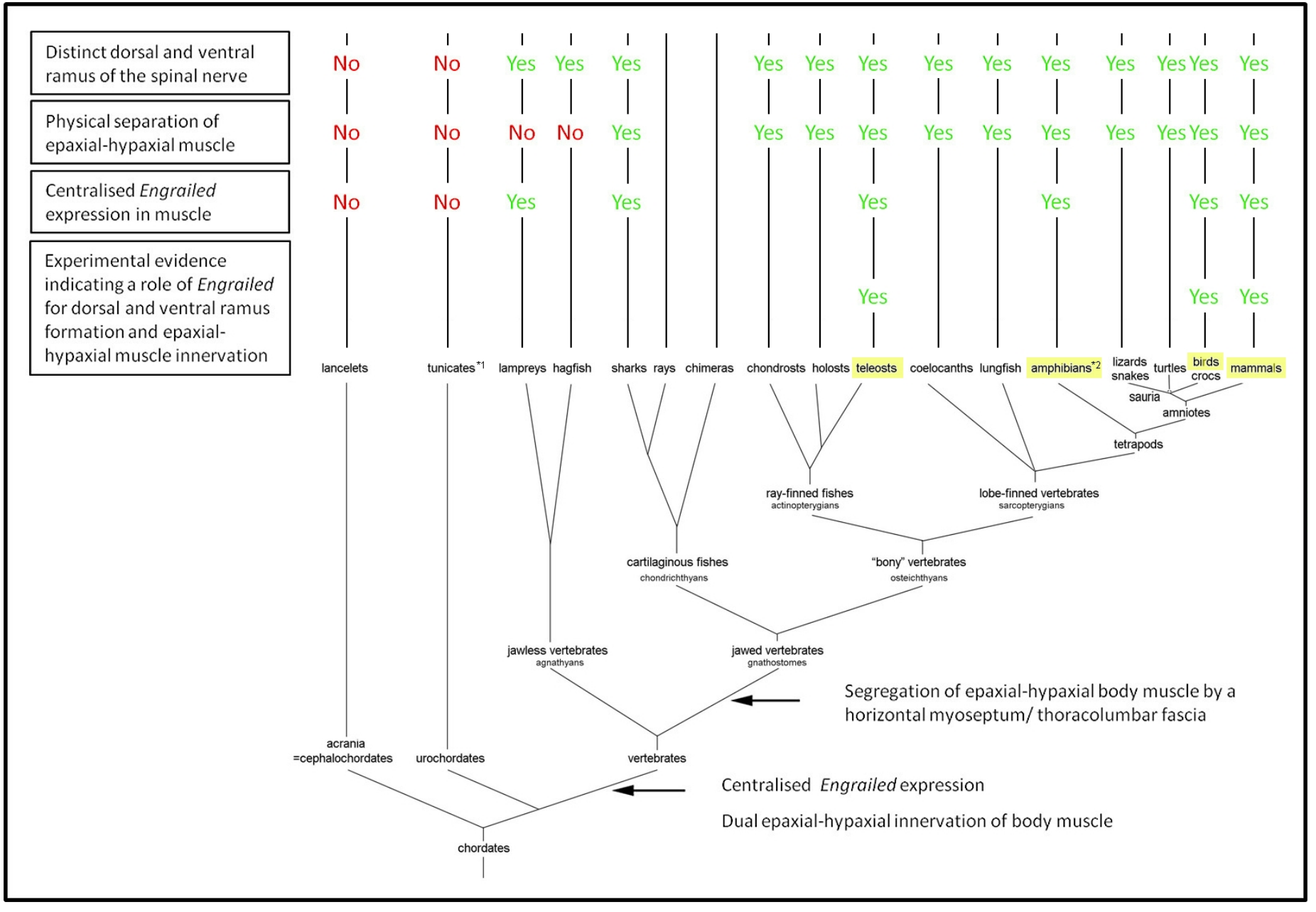
Distinct dorsal and ventral ramus of the spinal nerve
Physical separation of epaxial-hypaxial muscle
Centralised *Engrailed* expression in muscle
Experimental evidence indicating a role of *Engrailed* for dorsal and ventral ramus formation and epaxial-hypaxial muscle innervation
No No Yes Yes Yes Yes Yes Yes Yes Yes Yes Yes Yes Yes Yes
No No No No Yes Yes Yes Yes Yes Yes Yes Yes Yes Yes
No No Yes Yes Yes Yes Yes Yes Yes
Yes Yes Yes Yes
lancelets
tunicates*1
lampreys
hagfish
sharks
rays
chimeras
chondrosts
holosts
teleosts
coelocanths
lungfish
amphibians*2
lizards snakes
turtles
birds crocs
mammals
sauria
amniotes
tetrapods
ray-finned fishes
actinopterygians
lobe-finned vertebrates
sarcopterygians
cartilaginous fishes
chondrichthyans
"bony" vertebrates
osteichthyans
jawless vertebrates
agnathyans
jawed vertebrates
gnathostomes
Segregation of epaxial-hypaxial body muscle by a horizontal myoseptum/ thoracolumbar fascia
acrania =cephalochordates
urochordates
vertebrates
Centralised *Engrailed* expression
Dual epaxial-hypaxial innervation of body muscle
chordates